PROCEEDINGS, 42nd Workshop on Geothermal Reservoir Engineering
Stanford University, Stanford, California, February 13-15, 2017
SGP-TR-212

Tutuila, American Samoa: A Case History of Geothermal Exploration on a Deep Sea Island

Maxwell Wilmarth, Jill Haizlip and William Cumming

Geologica Geothermal Group, 5 Third Street, Suite 420, San Francisco 94103

mwilmarth@geologica.net

Keywords: American Samoa, exploration, island

ABSTRACT

Geothermal exploration on the island of Tutuila, American Samoa focused on a young extensional volcanic feature, the Holocene Rift Zone, which hosted the most recent eruption on the island, a ~600 year old basalt lava flow. Although a lack of fumaroles or hot springs implied that exploration would be relatively high risk, very high power prices led to an exploration program guided by a preliminary conceptual model including a sub-boiling reservoir with an outflow guided offshore by a clay cap, while a very high flux of meteoric water in the permeable lavas above the cap hid surface evidence of the reservoir. Geology, MT resistivity, CO_2-soil gas, soil chemistry and hydrology surveys were completed to indicate whether this or any resource model was plausible and to target relatively low cost temperature gradient holes. The deep low resistivity zone detected dipping up to the south beneath the coast was consistent with the model supporting a blind geothermal system and supported targeting of two temperature gradient holes continuously cored to ~600 m. The geology, alteration and temperature in these wells demonstrated that no geothermal system existed and that meteoric water apparently penetrated through the low resistivity clay zone, resulting in an unusually low temperature gradient. This case history demonstrates a relatively low cost strategy to test plausible but high risk geothermal prospects, such as isolated volcanic islands. This paper also highlights unusual conceptual aspects of exploration on relatively small volcanic islands like Tutuila.

1. INTRODUCTION

Geologica Geothermal Group Inc. (GEOLOGICA) was retained by the American Samoa Power Authority (ASPA) to evaluate the geothermal energy potential of the Territory of American Samoa, focusing on the main island of Tutuila. The justification for this work was ASPA's interest in the development of a geothermal reservoir as a power source for Tutuila which would reduce the high cost of current generation, chiefly diesel. This evaluation resulted in several phases of investigation between 2013 and 2016 culminating in drilling of two temperature gradient holes (TGH) in the youngest volcanic feature on the island, the Holocene Rift Zone (HRZ).

The use of geothermal conceptual models are the current best practice for geothermal resource assessment and well targeting (e.g. US-DOE, 2014; Cumming, 2016; Mortensen and Axelsson, 2013). Therefore, a staged program was devised to incrementally reduce the most commercially decisive sources of uncertainty in the resource conceptual models at a cost commensurate with the likelihood of discovering a commercial resource. The initial Phase 1 of this project focused on assessing whether any conceptual model for a developable geothermal reservoir was consistent with the initial background geoscience reviews and a preliminary surface review, particularly with respect to the lack of fumaroles and hot springs. Following the development of a plausible preliminary conceptual model, a Phase 2 set of surveys was conducted to build sufficient evidence for the key aspects of the model to justify targeting two or three low cost TGHs that would decisively test for high temperatures consistent with a commercial resource. If the TGHs were successful, depending on cost and perceived risk, drilling a testable slim hole or perhaps a production well might have been recommended. However, despite the potential for heat indicated by young volcanism in the HRZ, temperature gradients were below background and no evidence of extensive hydrothermal alteration was identified in the boreholes. Taken together, these and previous geoscientific results from this investigation of the geothermal potential of American Samoa support the conclusion that it is very unlikely that a commercial geothermal resource exists on Tutuila.

Published exploration case histories for geothermal exploration of analogous volcanic islands include several success cases and more inconclusive cases. There are very few (perhaps no) decisive failure cases, and there are no published exploration case histories for blind geothermal prospects on volcanic islands. Recent geothermal development in the Basin and Range suggests that exploration of blind geothermal systems can be commercially viable using phased exploration. Geothermal resource conceptual models are successively updated, initially using surface geoscience surveys that constrain targets for low-cost TGHs that constrain the thermodynamic model in a manner that either decisively eliminates the prospect at an economically viable cost or supports deep exploration drilling (Nordquist and Delwiche, 2013). The phased approach to exploration using successive surface studies supporting low-cost TGHs was adopted as the most cost-effective option for this project.

This paper presents a summary of the geothermal investigations and implications for geothermal potential on Tutuila with a focus on the geology and drilling results and how they fit the other data sets. Following a summary of the three Phases of the project, a review of the geology of Tutuila introduces the results of the core drilling. Brief reviews of how the drilling results fit with the other surveys support conclusions regarding all of the surveys conducted at Tutuila as part of the geothermal exploration program and their implications for geothermal exploration in analogous circumstances. This paper is largely drawn from the final report for the project (GEOLOGICA, 2016c).

2. PROJECT HISTORY

Phase 1

After a preliminary desktop study based on available geoscientific literature (GEOLOGICA, 2013), Phase 1 consisted of field work focused on identifying indications of a geothermal system, including soil and groundwater sampling, reconnaissance geologic and structural observations, a soil gas survey, and ground truthing of remote sensing data. The results of Phase 1 narrowed the focus of the investigation to the HRZ as the area of Tutuila with the highest probability of hosting both high-temperature fluid and permeability (GEOLOGICA, 2014a). The initial conceptual model for the success case devised by the GEOLOGICA team consistent with existing preliminary observations implied that a geothermal reservoir near the most recent eruption center did not produce surface manifestations because a thick, clay-rich cap diverted a hot sub-boiling outflow offshore so that most of the heat was hidden below the ocean. In this model meteoric water flushed through very permeable lavas above the clay cap, producing a chilled zone analogous to a similar zone sometimes called a "rain curtain" at the almost-hidden Glass Mountain Geothermal Field in California (Cumming and Mackie, 2007). In order to test this model and the potential of a geothermal system in the HRZ, additional surface studies were recommended for Phase 2.

Phase 2

Phase 2 consisted an aerial imagery review, LiDAR lineament mapping, further soil gas surveys, and a magnetotelluric (MT) resistivity survey. The results of Phase 2 were consistent with the most important aspects of the initial conceptual model for a possible geothermal system on Tutuila (GEOLOGICA, 2014b), demonstrating the existence of a low permeability clay zone that might cap a reservoir with an outflow directed offshore to the south. As expected, Phase 2 did not detect direct evidence of commercial temperature but it did support targeting of low-cost temperature gradient wells that would greatly reduce risk of any potential production well drilling by confirming or discrediting the hypothesis of a high temperature reservoir hidden below the clay cap.

The conceptual model for a geothermal system underlying the HRZ included hot fluid upflow deep within the HRZ diverted by a caprock southward into submarine outflows of hot water (GEOLOGICA, 2014b). The caprock in the model was interpreted as the almost flat-lying low-resistivity zone imaged in the MT survey as dipping slightly up to the south toward the coast, consistent with an outflow in that direction. The geometry and characteristics of this conductor were consistent with volcanics with clay alteration or, closer to the coast, more likely saltwater-saturated volcaniclastic or sedimentary rocks with intercalated clay-rich zones. In either case, the low resistivity zone seemed likely to correspond to low-permeability rocks, with both resistivity and permeability potentially further reduced by hydrothermal clay alteration.

The geometry of the low-resistivity rocks imaged in the MT survey were consistent with the interpretation of hydraulic cap on a geothermal reservoir required for an active geothermal system to exist with no apparent surface thermal features. However, alternative models implied that the risk remained too high to justify targeting a production well. None of the surveys could confirm the existence of high temperature beneath the low resistivity cap. The low-resistivity zone could have been related to saltwater-saturated sediments beneath the volcanic edifice or to relict alteration from a former geothermal system now cooled. Although the lack of geothermal surface manifestations might be consistent with the proposed conceptual model, it was still more likely that the source of the young volcanics and related magmatic gas emissions were too deep and/or too small to produce a geothermal system. If the low-resistivity zone was functioning as a hydraulic cap above a geothermal system, then heat from the geothermal system would create a conductive thermal gradient through the cap which would separate the surface volcanics chilled by surface meteoric water from the hot resource below the cap. Given the dip of the cap, it should deflect the hot water to locations where the gradient in the cap could be measured by relatively low-cost 600 m deep TGHs. A low temperature gradient in the low resistivity section would be decisively negative, whereas a gradient indicating temperatures of at least 120°C in the outflow might justify targeting a production well. By targeting the caprock rather than the geothermal reservoir, the risk of encountering geothermal fluids was reduced and therefore drilling and related environmental risks were also reduced. If this zone overlaid a geothermal system, the temperature gradients in the low-permeability zone would be significantly higher than background. Therefore, the temperature gradient holes targeted this low-resistivity zone.

Anomalous levels of carbon dioxide (CO_2) and radon detected in soil gas on either side of the HRZ were interpreted as a possible lateral subsurface outflow of hydrothermal fluids from an upflow in the HRZ.

Phase 3

Phase 2 resulted in selection of drilling targets within and adjacent to the HRZ that could be used to test the conceptual models. Specifically, plans were developed to construct boreholes allowing temperature surveys (temperature versus depth measurements) and hydrothermal mineralogical evaluation of core and cuttings to test whether the temperature gradients and hydrothermal alteration mineralogy within the boreholes were consistent with the low-resistivity zone representing a geothermal cap (GEOLOGICA, 2015).

Phase 3 included drilling two TGHs in the area of the HRZ to depths of ~2,200 feet, which was a depth attainable by cost-effective diamond coring drill rigs and deep enough to measure the geothermal gradient within the low-resistivity zone and below the influence of cold surface waters. Additionally, the TGH program included logging borehole geology and temperatures, laboratory analysis of core samples, and relating the borehole geology to the mapped surface geology. TGH-1 was drilled in the western portion of the HRZ in Malaeloa Valley while TGH-3 was drilled in the eastern portion of the HRZ in the village of Ili'ili (Figure 5). The two TGHs are the only boreholes on Tutuila deeper than ~300 ft.

These boreholes did not encounter mineralogy or temperatures indicative of a geothermal system. TGH-1 drilled through ~100 ft of Taputapu Volcanics deposited as erosional material before encountering >100 ft of Leone Volcanics. Leone carbonate reef deposits may

have been present below this depth but a lost circulation zone (where drilling mud is lost to formation) resulted in no returns before coring resumed; therefore, no lithologic identification was possible in that zone. When coring resumed in TGH-3, the rocks were paleo-deposited Taputapu-derived sediments and in-place Taputapu Volcanics. TGH-3 cored ~500 feet of the younger Leone Volcanics and carbonate reef before encountering redeposited volcanics and the older in-place Taputapu Volcanics. Alternating sequences of basaltic lava flows and clay-rich volcaniclastic units in both TGHs suggest that horizontal permeability is high within fractured basalt flows while vertical permeability is very low and limited by the clay-rich volcaniclastic units. Vertical permeability could be higher where the stratigraphy is cut by high-angle fractures and normal faults, which were observed in the core of both TGH-1 and TGH-3, associated with the HRZ. Alteration mineralogy is dominated by low-temperature smectite, kaolinite and zeolite clay minerals in both TGHs. Maximum temperatures measured in the TGHs were ~37°C at the bottom of each of the boreholes. The conductive geothermal gradient is ~20-25°C/km, consistent with the worldwide crustal average. Given the lack of evidence for a geothermal system in the first two TGHs, TGH-2, planned for the middle of the HRZ, was not drilled.

3. REGIONAL GEOLOGY

The Samoan Archipelago is a South Pacific island chain (Figure 1) originally formed by hotspot volcanism. Age dating of dredged basalts from seamounts indicates the age of the Samoan hotspot lineament ranges from ~24 million years ago (Mya) for the submerged Alexa bank at the western extreme of the chain, to present day for the currently active Vailulu'u seamount (Figure 2) at the eastern end (Hart et al, 2004). The islands of the archipelago, both those submerged and those currently above sea level, are progressively younger from west to east, although recent (Holocene) rejuvenated volcanism has given the western islands a more youthful appearance (Keating, 1992). The temporal confusion caused by rejuvenated volcanism in the oldest (western) part of the island chain has led some workers to question the hot spot model (e.g. Natland, 1980). Westward plate motion has been estimated at 7 cm (Hart et al., 2004) to 10 cm per year (McDougall, 1985). American Samoa, a Territory of the United States, occupies the eastern and younger portion of the island chain. The largest and westernmost island of American Samoa, Tutuila (Figure 2), is a deeply eroded, sinuous island approximately 3 miles wide (north to south) and 20 miles long (west to east), built from several shield volcanoes along an ENE alignment which coalesced ~1 to 1.5 million years ago as deduced from Potassium-Argon age dating (McDougall, 1985). The shield-forming lavas have tholeiitic to alkali petrology reflecting heterogeneous upper mantle chemistry beneath the Samoan Archipelago, which is depleted in trace elements (Natland and Turner, 1985).

After a long period of erosion and subsidence (~1 million years), volcanism on Tutuila was rejuvenated in the Holocene, possibly related to subduction at the nearby Tonga Trench and tearing of the oceanic plate during oblique flexure (Keating, 1992), and continued until as recently as 600 years ago, constrained by archaeological evidence and radiocarbon dates (Addison et al., 2014). The recent volcanism was focused along the HRZ, a north-south lineament of young volcanic cones and craters, with associated high-angle normal faults and fractures, on the Tafuna-Leone Plain in southwestern Tutuila. The HRZ was first described as a rift zone by Stearns (1944) and is interpreted by GEOLOGICA to be either a volcanic fissure ridge or rift zone. The young Leone lavas, when compared to the older shield-forming volcanics, are relatively depleted in silica and appear to originate from a different magma source (Natland and Turner, 1985). They are relatively unweathered compared to the older Pleistocene volcanics, consisting of lava flows, cones and craters with minimal erosion. Despite the potential for a nearby heat source presented by this young volcanism, no thermal manifestations such as hot springs, fumaroles, or sinter have been reported on Tutuila.

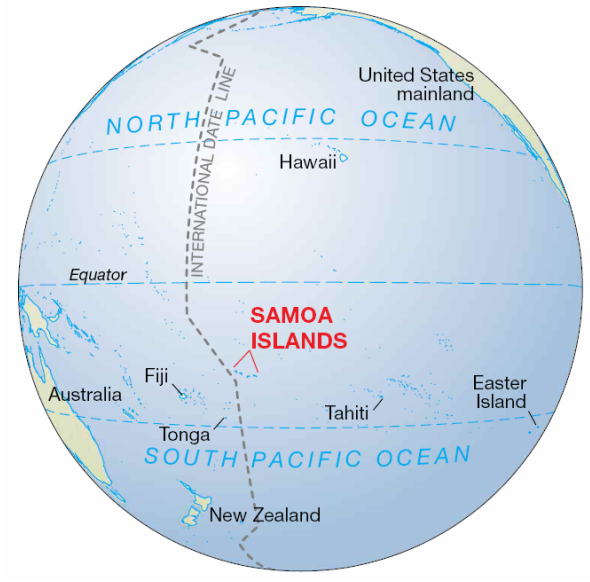

Figure 1. Location of the Samoan Islands in the South Pacific, from NPS (2008).

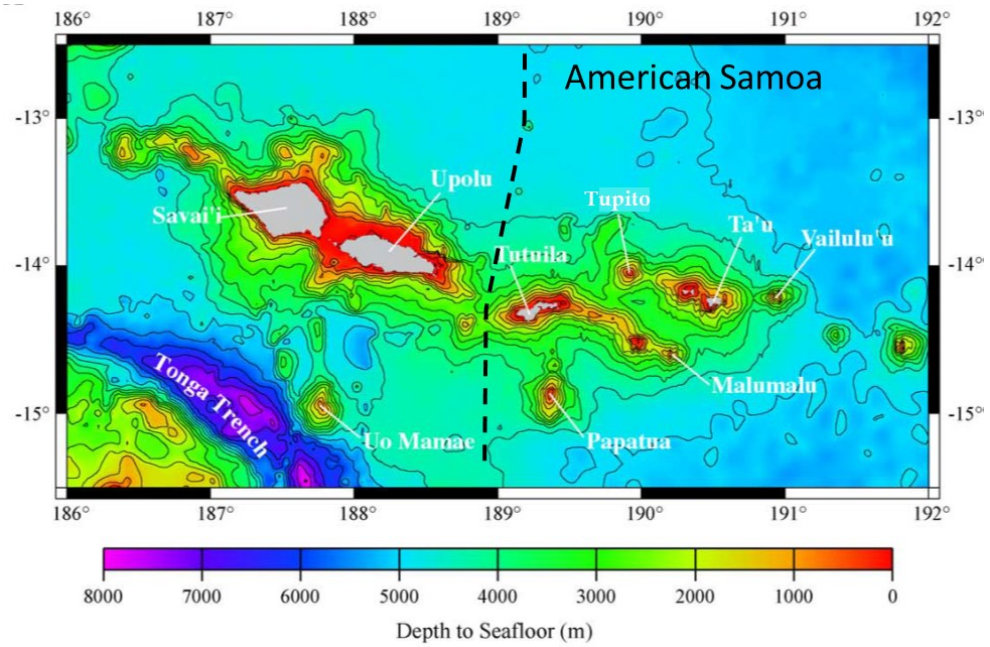

Figure 2. Bathymetric map of the Samoan Islands showing modern political divisions and the location of the Tonga Trench, after Hart (2004).

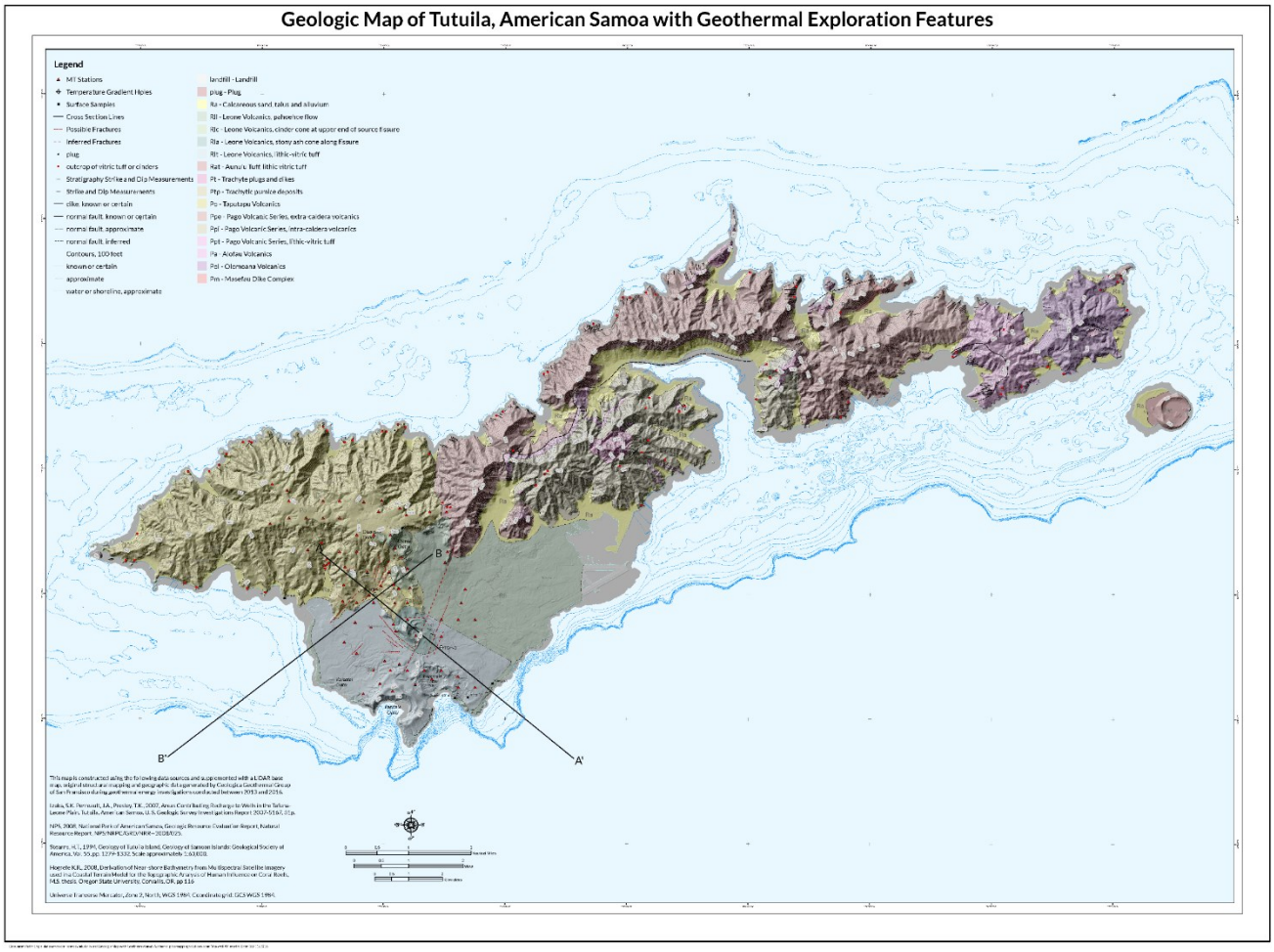

Figure 3. Geologic Map of Tutuila with Geothermal Exploration Features. Cross sections AA' and BB' are shown below. Basemap is LiDAR topographical model.

4. BACKGROUND GEOLOGY OF THE TAFUNA-LEONE PLAIN

The Tafuna-Leone Plain forms a peninsula dominating the southwest sector of Tutuila. This broad peninsula is covered at the surface by Holocene-age Leone Volcanics extending approximately one mile offshore to the south (Eyre and Walker, 1991). The vents for the Leone Volcanics are concentrated along a 2 to 3-mile long rift (Stearns, 1944) known as the Holocene Rift Zone (HRZ). The HRZ extends from the large Olotele cinder cone in the north, to the Fagatele tuff cone in the south (Figure 3, Figure 5). Recent bathymetry (Hogrefe, 2008) of the seafloor around Tutuila indicates that there may be submerged vents that continue offshore to the south of the Tafuna-Leone Plain. Numerous lineaments interpreted to be extensional normal-faults and fractures have been mapped by GEOLOGICA (GEOLOGICA, 2013). The Leone Volcanics issued from three tuff cones: Fogamaa, Fagatele and Vailoatai, and two cinder cones east of Maupasaga including Olotele Peak and the stony ash cone at Futiga (Stearns, 1944). Several of these craters, including Futiga, were formed when lava flowed into seawater, causing explosions. Lava eruptions from this fissure ridge erupted significant volumes of mafic lavas and related airborne volcanic material during a relatively short period during the Holocene. Leone volcanic flows may have continued until as recently as ~600 years ago, constrained by archaeological evidence and radiocarbon dates (Addison et al., 2014).

The uppermost rocks in the lithologic sequence of the Tafuna-Leone Plain cover most of the surface, and are composed dominantly of shallowly dipping vesiculated pahoehoe basaltic lavas (Figure 6) alternating with tuffs and basaltic volcaniclastic sediments (Figure 7). These lavas are classified as picritic basanites with up to 15 to 20% olivine and clinopyroxene ± plagioclase microphenocrysts (Hawkins and Natland, 1975).

Lava flows within the Leone Volcanics are permeable and constitute the dominant groundwater aquifer on Tutuila (Eyre and Walker, 1991). Locally, and generally in the highlands above the plain, groundwater can be impounded in small dike-bounded reservoirs perched above the regional groundwater table (Davis, 1962).

Leone Volcanics are related to the "post-erosional" or rejuvenated-stage (Natland, 1980; Hart et al., 2004) of volcanism in the Samoa Islands, as distinguished from the older hot-spot-related shield-building volcanics, which built most of the Samoan islands, including Tutuila (Hawkins and Natland, 1975; Natland, 1980; Natland and Turner, 1985). However, the rejuvenated volcanism of Tutuila and Western Samoa does not appear to represent the rejuvenation of the hot spot activity which built the islands, but is instead reported to be related to the location of these islands relative to the terminus of the Tonga Trench and the related subduction, tearing and oblique flexure (Hawkins and Natland, 1975; Natland, 1980; Hart et al., 2004). The rejuvenated volcanics of the Tafuna-Leone Plain are silica-depleted basanites, which can be distinguished from the shield-building alkali basalts by rock chemistry and mineralogy. Leone Volcanic rocks are low in silica and alumina-oxide relative to the older pre-erosional volcanics and have olivine and clinopyroxene ± plagioclase microphenocrysts. The older hot-spot related shield lavas are lower in total alkali ($Na_2O + K_2O$ wt% relative to SiO_2) and the different isotopes of various elements such as Pb and Sr (Konter and Jackson, 2012). Consistent with other rejuvenated-stage Samoan Volcanics, Leone Volcanics were reported to have 43.2-43.7 wt% SiO_2 and 3.4-4 wt% $Na_2O + K_2O$ (Hawkins and Natland, 1975), as shown in Figure 4.

The chemistry and mineralogy suggest that the magmatic sources of the Leone Volcanic rocks and the older volcanics were different. Though the source of the rejuvenated magma which forms the Leone Volcanics may have a lithospheric component (Hart et al., 2004; Konter and Jackson, 2011), the older hot-spot shield-building volcanics could have had a deeper source. The magma that produced the rejuvenated volcanics probably originated at a depth of around 90 km (Konter and Jackson, 2011). Magma sources of this depth rarely provide heat for geothermal systems within drillable depths (usually 2 to 3.5 km) unless they are very young (<1000 years) or remain hot enough at shallow depths in dikes, magma chambers or other related features. Because the rejuvenated volcanics of Samoa (and Tutuila) reportedly rose quickly to the surface from a maximum magma residence depth of about 15 to 20 km (based on phenocryst growth; Hawkins and Natland, 1975) without any significant accumulation or residence time in the shallow crust that might provide a magmatic heat source, they could supply the heat for a geothermal system only if they are very young.

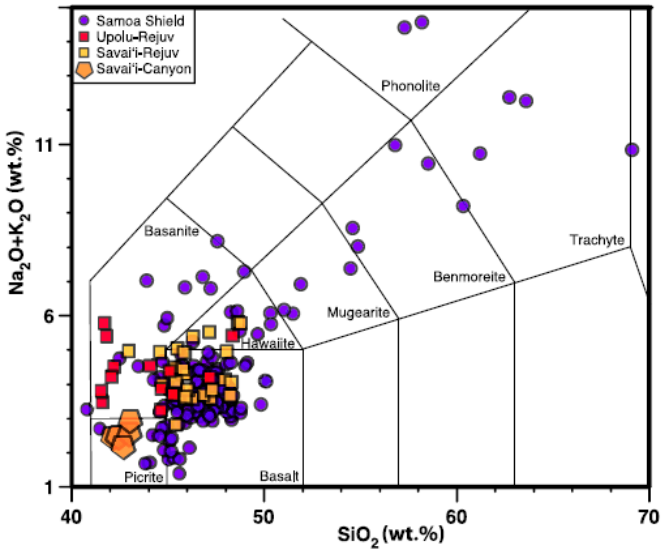

Figure 4. Silica (SiO_2) versus alkalis ($Na_2O + K_2O$) in Samoan Volcanics. Shield volcanics are presented as purple circles, rejuvenated volcanics are the orange squares, red squares and pentagons, from Konter and Jackson (2011). Blue "X" represents Leone Volcanic chemistry, average of four basanites, from Hawkins and Natland (1975).

The stratigraphically lower and older Pleistocene Taputapu Volcanics, exposed on the western coastal and northern upland margins of the plain (Symbol "Po" in Figure 3) underlie the Leone Volcanics. Taputapu Volcanics are one of the four or five major shield-building alkali basalts volcanoes (the others are Masefau, Olomoana, Alofau and Pago Pago) which formed Tutuila along a N70°E trend between approximately 1.01 and 1.54 million years ago (McDougall, 1985). Between the eruption of Leone and Taputapu Volcanics, there was a long period of deep erosion, deposition and reef building, which produced volcanogenic sediments, beach sands and reef-related carbonates. Taputapu Volcanics can be found stratigraphically above Leone Volcanics where Taputapu Volcanic material has eroded from the upper slopes and been deposited on top of Leone Formation as recent sediments (Eyre, 2016).

The Taputapu Formation generally consists of olivine basalt flows 2 to 15 m thick and dipping <20° towards the paleo-coastline (Keating, 1992). The contact between Leone Volcanics and Taputapu Volcanics was modeled by Eyre and Walker (1991) and generally mirrors the current topography. As Tutuila subsided into the ocean during the Pleistocene and after the end of the shield-building phase, carbonates and sediments accumulated on the margins of the platform. Subsequent to rapid Holocene sea level rise, reef-forming corals were covered by erupting Leone Volcanics and are included in the Leone Formation in the boreholes. These carbonates have been observed both offshore (Wright et al, 2012) and were encountered in TGH-3.

Table 1. Geologic units found on the Tafuna-Leone Plain. Map unit symbols refer to map in Figure 3 and Figure 5.

Period	Epoch	Epoch Date Range (years B.P.)	Map Unit (Symbol)	Unit Description
Quaternery	Holocene	Present to ~11,700	Sedimentary Rocks (Ra)	Modern soils derived from underlying Leone Volcanincs and shed from ridges.
				Talus at the foot of valley walls and river deposited alluvium on valley floors (NPS, 2008).
			Leone Volcanics (Rll)	Rll contains olivine pahoehoe basalt flows (NPS, 2008).
			Leone Volcanics - Stony ash (Rla)	Rla contains deposits of stony ash along the source fissure zone (NPS, 2008).
			Leone Volcanics - cinder cone (Rlc)	Rlc consists of cinder cone deposits localized at the upper (northern) end of the source fissure (NPS, 2008).
			Leone Volcanics - lithic/vitric (Rlt)	Rlt contains at least 2 thick tuff beds from Vailoatai, Fagatele, and Fogamaa Craters with material from Fogama'a Crater atop the Fagatele Crater volcanic deposits (NPS, 2008).
			Leone Carbonates + Volcanics [No surface outcrops]	Shallow carbonate reefs and marly clays interbedded with Leone Formation lava flows and volcaniclastics. Formed when sea levels rose ~400 ft at beginning of Holocene (Eyre, 2016).
	Pleistocene	~11,700 to 2.6 Million	Pleistocene Carbonates + Sediments [No surface outcrops]	Pleistocene reef and sediment platform built on the flank of Taputapu volcano, growing towards the ocean surface as Tutuila subsided ~2,500 ft. The material is both depositional (terrigenous and marine) and wave-cut, depending on the changing relationship between fluctuating Pleistocene sea levels with the shoreline of the subsiding island (Eyre, 2016).
Neogene	Pliocence	~2.6 to 5.3 Million	Taputapu Volcanics (Po)	Undifferentiated olivine basalts (2 to 15 m thick), dipping 5°- 10° from a rift zone parallel to the Samoan Ridge interlayered with thin- bedded cinder cone deposits, dikes, and thin vitric tuff beds. In some areas the volcanics are capped by thicker flows of porphyritic and nonporphyritic olivine poor basalts. Some red vitric tuff and cinders present locally (NPS, 2008).

B.P. = Before Present

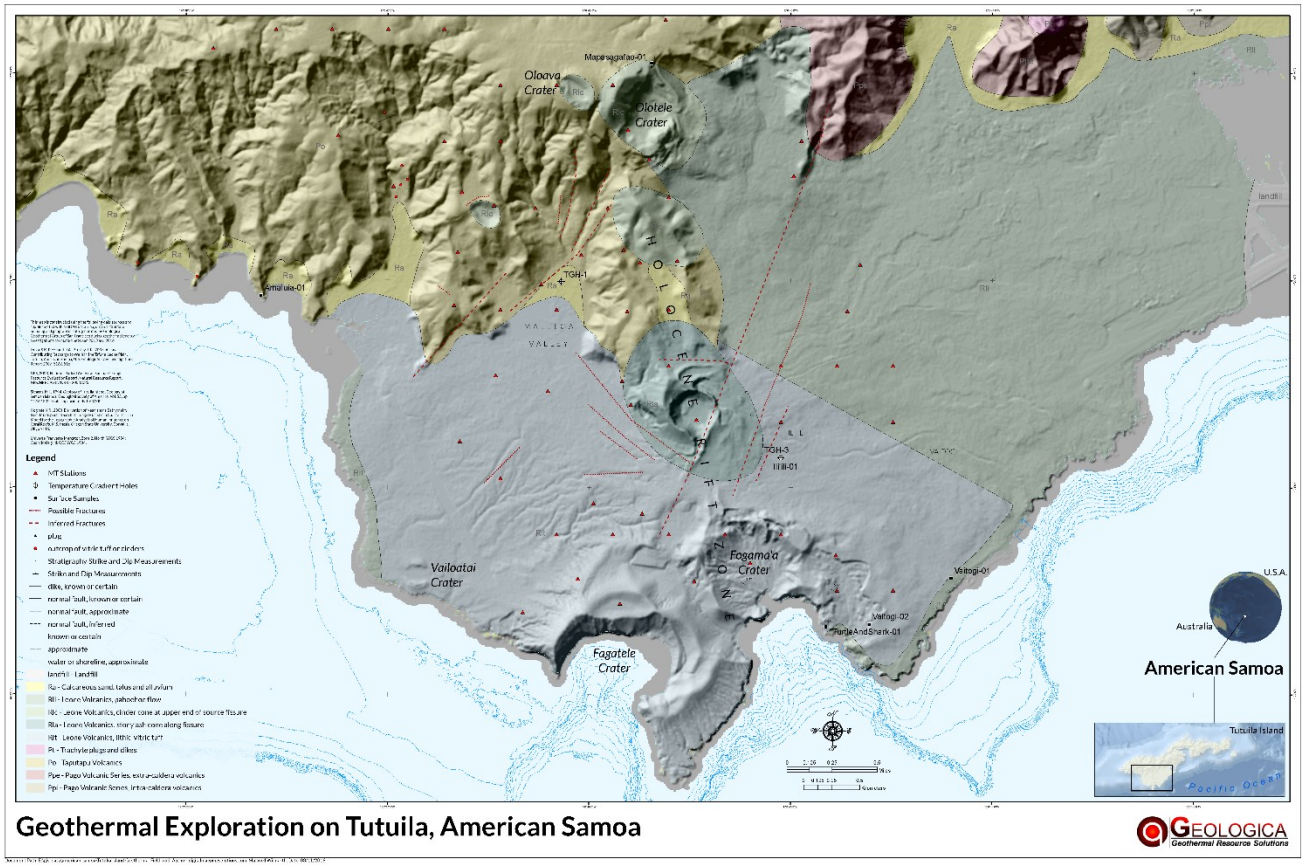

Figure 5. Inset map of the Tafuna-Leone Plain with HRZ labeled. Basemap is LiDAR topographical model.

Figure 6. Shallow-dipping Leone Volcanics, basalt flow along the south shore of Tutuila, west of the village of Vaitogi.

Figure 7. Low-angle bedding in Leone Volcanic ash with soft-sediment deformation around vesicular basalt lava clast, on south shore below Turtle and Shark hotel. The volcaniclastic layers are composed of glassy ash, fine lapilli, and granulated rocks that are easily converted to clay in the tropical environment.

5. PHASE 3 INVESTIGATION

Phase 3 included TGH drilling originally planned as a two to three hole program with the third hole contingent on preliminary results from the first two. Surface field geology work was conducted to correlate borehole geology with mapped units. Summary lithologic and borehole construction logs are included here for TGH-1 and TGH-3 (Figure 8 and Figure 9). TGH-2 was not drilled because of the lack of hydrothermal alteration mineralogy and the low temperatures encountered in the first two TGHs.

5.1. Temperature Gradient Hole Targeting Rationale

The TGH targets were selected to test the hypothesized conceptual model of a geothermal system on Tutuila (GEOLOGICA, 2014b). The original conceptual model from Phase 2 posited that despite the lack of surface thermal features, the most likely location for a geothermal reservoir on Tutuila was beneath the HRZ. If the electrical conductor observed in the 2014 MT survey represented an impermeable caprock layer, hot upflowing fluid within the HRZ would be diverted southward to submarine outflows explaining the lack of surface manifestations. The TGH targets were specifically designed to measure the temperature gradient in the low-permeability possible caprock zone, where the temperature gradient would be elevated above the background gradient in the presence of an underlying geothermal system.

Variations in carbon dioxide and radon concentrations measured in the near-surface soil were mapped on the Tafuna-Leone Plain and in the HRZ during Phase 1 site investigations (GEOLOGICA, 2014b). Anomalous concentrations were identified in several areas adjacent to the HRZ, which were identified as possible outgassing from deep lateral outflows from a geothermal system upflowing within the axis of the HRZ. The TGHs were targeted to test for elevated temperature gradients associated with these areas.

5.2. Drilling and Borehole Construction

TGH-1 and TGH-3 were drilled by West-Core Drilling of Elko, Nevada with a track-mounted Atelier Val'Dor Deep Hole Core Drill. Rotary tools were used in the shallow subsurface followed by diamond core tooling to recover continuous core.

TGH-1 was drilled in September and October 2015 at a location in the western portion of the Tutuila HRZ in Malaeloa Valley (Figure 5) at a ground elevation of ~125 ft above mean sea level (msl). The wellhead location is (WGS84) 14.3335° S, 170.7690° W. TGH-1 was drilled primarily with HQ core rods to a total depth (TD) of 2,176 ft below ground surface (bgs).

TGH-3 was drilled in October and November 2015 at a location in the eastern portion of the HRZ in the village of Ili'ili (Figure 5) at a ground elevation of ~252 ft above msl. The wellhead location is (WGS84) 14.3368° S, 170.7685° W. TGH-3 was drilled to a total depth of 2,117 ft with HQ core rods.

BQ rods were hung from the surface to TD in both TGH to facilitate temperature logging.

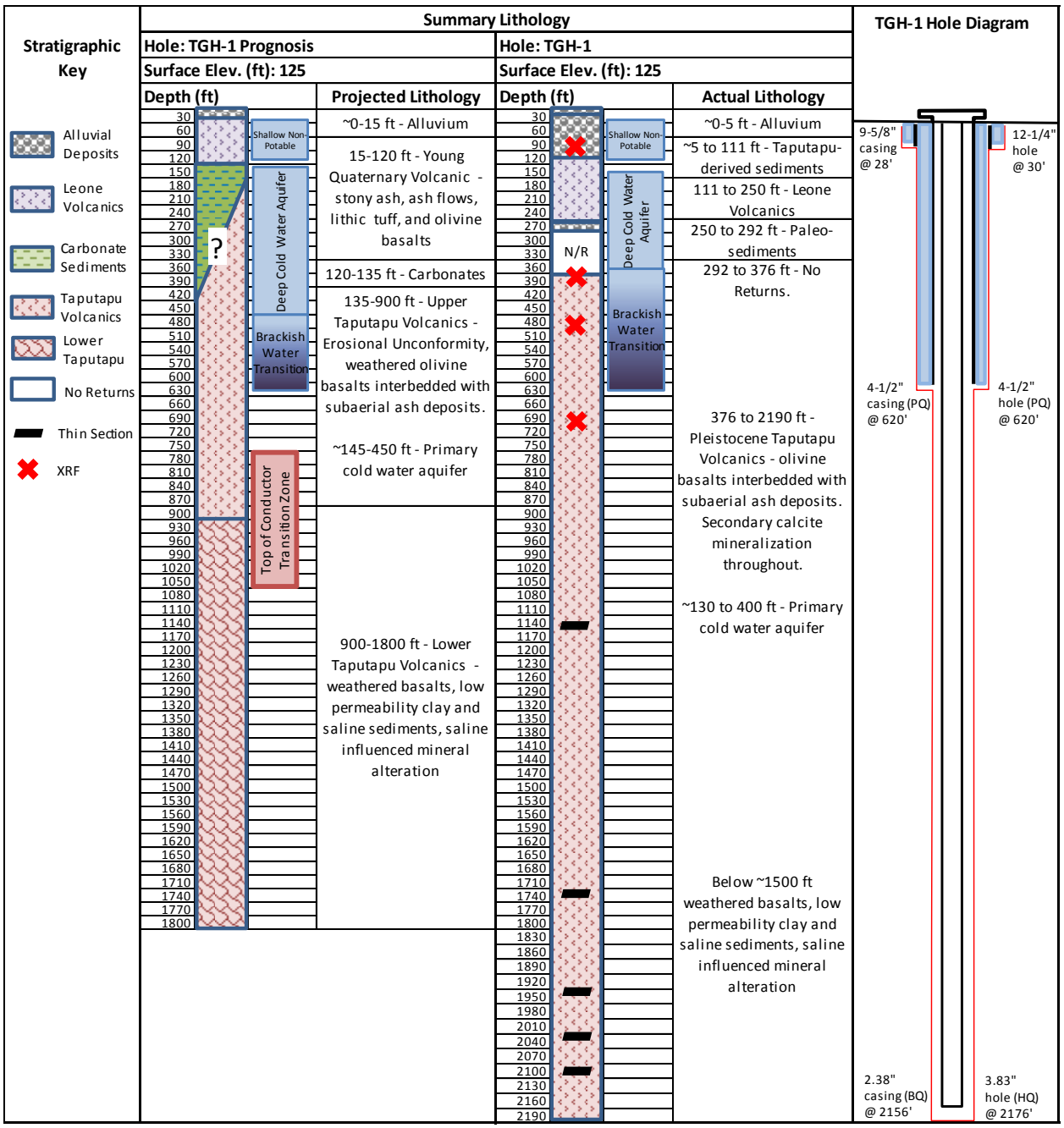

Figure 8. TGH-1 summary log of borehole construction and projected vs actual lithology.

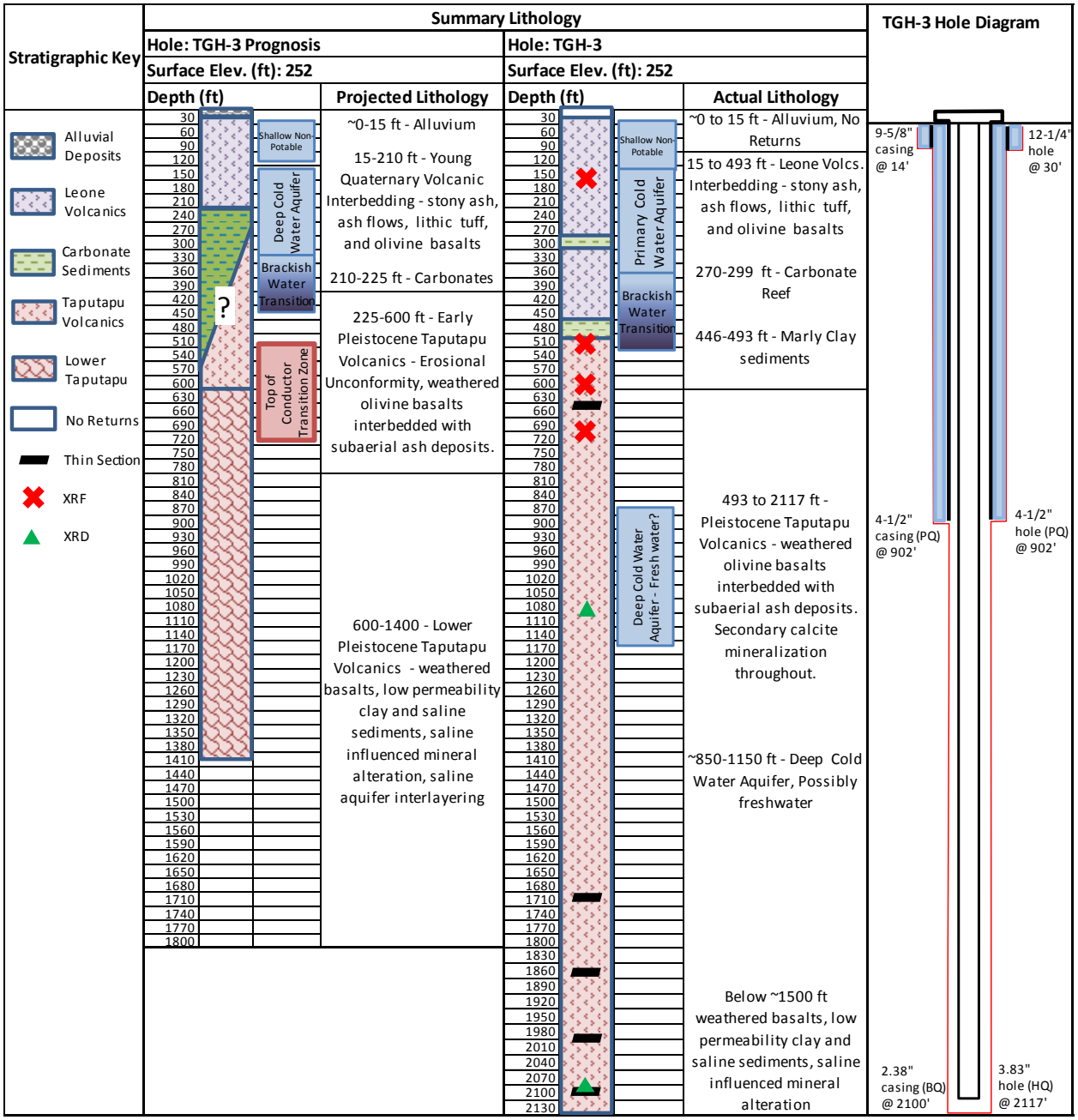

Figure 9. TGH-3 summary log of borehole construction and projected vs actual lithology.

5.3. Core Logging

Well-site geology was provided by GEOLOGICA. A summary comparison of the lithologic prognosis and actual lithologic log is presented below. Detailed core logs can be found in GEOLOGICA (2016c).

5.3.1. Lithology

Lithology of core and cuttings was evaluated in the field using visual inspection and microscope evaluation by the wellsite geologists. Core and cuttings samples were logged by depth and are stored in the ASPA offices on Tutuila. Lithologic descriptions were recorded in ~1 ft increments.

The expected sequence in both TGHs was Holocene Leone Volcanics and reef carbonates underlain by the Pleistocene Taputapu Volcanics loosely divided into Upper and Lower units, based on apparent resistivity differences in the MT data. It should be noted that this stratigraphic column was derived largely from surface geologic mapping and shallow groundwater well logs as no deep (>300 ft bgs) drilling had previously occurred on Tutuila.

TGH-1

The interval from 0 to 89 ft bgs was drilled with a tricone bit, resulting in pulverized cuttings rather than intact core. TGH-1 encountered alluvial fill consisting of reddish-brown clayey material from 0-5 ft bgs. From this depth to TD, drilling encountered a sequence of volcanic and volcaniclastic sediments (Figure 10) logged variously as tuffs, debris flows, breccias, and scorias, with occasional paleosols. Consultation with Paul Eyre (June, 2016) resulted in re-interpreting the interval from 5 to 125 ft as sediments ranging up to boulder-size and from 125 to 250 ft bgs as Leone Volcanics. No primary carbonate units were observed in the core; carbonate was only observed as secondary calcite mineralization. A zone of total lost circulation with no returns was drilled from 292 to 376 ft bgs.

TGH-3

TGH-3 encountered immediate total losses from the surface but appears to have drilled alluvial fill from 0-15 ft bgs. Below 15 ft bgs, enough core was recovered to log lithology. The rocks encountered throughout TGH-3 are similar to TGH-1, with the exception of carbonates observed above 493 ft bgs. From 15-493 ft bgs drilling encountered a lithologic sequence of alternating basaltic lava flows and volcaniclastic sediments logged variously as tuffs, debris flows, breccias, and scorias, with occasional paleosols (Figure 10). Carbonate reef structures (corals) were encountered from 270-299 ft bgs (Figure 10) and marly clays were encountered from ~446-493 ft bgs. The rocks above 493 ft bgs are assigned to Leone Volcanics, and rocks below the base of the marly clays at 493 ft bgs are designated as Taputapu Volcanics, but the lithologies are very similar and are difficult to distinguish in the field using visual inspection and microscope evaluation.

Figure 10. Lithology from the two TGH. Top Left: Young Leone Volcanics basalt flows from ~ 220 ft bgs (TGH-1). Top Right: Taputapu Volcanics debris flow at ~600 ft bgs, highly altered by Fe-clays and hematite (TGH-1). Bottom Left: Leone Carbonates reef structures at 295 ft bgs (TGH-3). Bottom Right: Taputapu Volcanics olivine basalt at 1329 ft bgs (TGH-3).

5.3.2. Structure

Lava flows in the cores of both TGHs range from massive and unfractured to highly fractured. Low-angle flow banding (<20°) is observed in basalts throughout the core from both TGHs (Figure 11). The volcaniclastic units range from massive to brecciated.

Highly fractured zones are common in low-strength units such as unsilicified ash flow tuffs. Primary porosity of the lavas, as with most fine-grained volcaniclastics, is very low except in vesiculated lava flows (Figure 11). However, there is abundant secondary permeability in rubbly breccia zones and in fractured lava flows.

Fracture density ranges from rare to common with dips ranging from near-horizontal to nearly vertical and from hackly and rough to highly planar. Since the core is not oriented, there is no way to determine the dip direction of the flows or the fractures. Fractures in both TGHs are variably open and vein-filled. Fault planes with slickensides, some of which bear alteration minerals, are present in both

TGHs, with high-angle to nearly vertical (parallel to the length of the core) dip-slip orientation. Slickensides were observed in TGH-1 at approximately 605, 1650, and 2030 ft bgs; and in TGH-3 at approximately 504, 1300, 1554, and 1923 ft bgs.

Figure 11. Details of structure in the core. Top Left: Horizontal flow banding at 1,482 ft bgs (TGH-1). Top Right: Dipping vesiculated bedding planes in lava flow (TGH-3). Bottom Left: Fractured lava flow with high-angle fractures and dip-slip slickensides at ~2,030 ft bgs (TGH-1). Bottom Right: High porosity in vesiculated lava flow at 1,413 ft bgs (TGH-3).

5.3.3. Alteration

Alteration in core from both TGHs is dominated by low-temperature argillic mineral assemblages including kaolinite + limonite + calcite + hematite (Figure 12). The alteration level varies widely from almost nonexistent in very fresh looking black basalt lavas (Figure 12), to intensely altered red iron (Fe)-clays in porous volcaniclastic materials (Figure 12), often oscillating back and forth over feet or inches. Phenocrysts, especially of feldspar, are preferentially altered to white clays. Alteration minerals preferentially fill veinlets, vesicles, and any other open space. Zeolites first appear in abundance at ~500 ft bgs in both TGHs, generally becoming more common with depth, especially below ~1,500 ft bgs. Zeolite mineral texture ranges from radiating acicular clusters of needles, to microscopic sucrosic clusters, to vein-filling massive crystals. Gypsum and/or anhydrite also appear in association with zeolites including megacrysts (4-5 inches in diameter) below ~1,500 ft bgs (Figure 12).

Figure 12. Details of core. Top Left: Brown limonite alteration of clay-rich volcaniclastic at 1,607 ft bgs in TGH-3 Top Right: Kaolinite-serpentine clays coating high-angle fracture at 1,860 ft in TGH-3. Bottom Left: Dog-tooth zeolite crystals at 2,021 ft bgs in TGH-3. Bottom Right: Massive gypsum megacryst filling open space at 2,097 ft bgs in TGH-3.

5.4. Laboratory Analysis

GEOLOGICA collected samples from the core of both TGHs for laboratory analysis by GNS Science in Taupo, New Zealand. The primary purpose of this analysis was to evaluate possible changes in the core due to water/rock interaction and, specifically, to assess the possibility that any observed changes might indicate the presence of higher temperature (higher than measured in the boreholes) water/rock interaction. The secondary objective was to support the lithological logging of the core based on visual and microscopic analysis in the field.

Analyses performed included thin-section preparation and description from polarized light microscope observation, whole-rock geochemistry including major and minor element abundances using X-ray fluorescence (XRF), clay analysis using Short-wave Infrared (SWIR) spectroscopy, and follow-up clay analysis using X-ray diffraction (XRD). Samples collected and the analyses performed are summarized below in Table 2. Additionally, six surface samples were collected for analysis by XRF in order to compare to the core samples. Surface samples collected and their locations are summarized in Table 3. All laboratory reports can be found in GEOLOGICA (2016c).

Four samples of Leone Formation carbonate from TGH-3 core were taken by University of California, Santa Barbara PhD candidate Andrew Reinhard and analyzed for Carbon-14 age dating at the Keck Carbon Cycle Accelerator Mass Spectrometry (UCIAMS) facility at the University of California, Irvine. This data set was provided to GEOLOGICA by ASPA as unpublished results (Reinhard, 2016).

Table 2. TGH core samples and analyses.

Sample Depths (ft bgs) by Laboratory Analysis						
TGH-1		TGH-3				
Thin Sections	XRF	Thin Sections	XRF	XRD	SWIR	14C Age Dating
1156	87	645	160	1100	33 samples from 242'-2100'	274.25^
1741	387	1716	254*	2100		295.5^
1950	494	1860	307*			298^
2032	696	1998	492*			453^
2104		2097	503*			
			505			
			618			
			703			
			1146*			

All Samples Collected by GEOLOGICA and Analyzed by GNS Science unless noted.

*Samples Collected by Paul Eyre and Analyzed by University of Hawaii

^Samples Collected by Andrew Reinhard and Analyzed at University of California, Irvine

Table 3. Surface samples analyzed by XRF and location.

Surface Samples Analyzed by XRF Samples Collected by GEOLOGICA and Analyzed by GNS Science			
Name	Rock type	WGS84	
		Latitude	Longitude
Ili'ili-01	Leone Basalt	-14.3476	-170.7509
TurtleAndShark-01	Leone Basalt	-14.3612	-170.7471
Amaluia-01	Taptapu Basalt	-14.3159	-170.7615

5.4.1. XRF

Four samples of core from TGH-1 and four samples from TGH-3 were analyzed at GNS by XRF for major and minor element concentrations. In addition, five samples were analyzed by XRF at the University of Hawaii (UH) and provided to GEOLOGICA by ASPA as unpublished results (Eyre, 2016). Competent and relatively unaltered lava samples were selected from the core by GEOLOGICA. Three surface outcrop samples of mapped Leone Volcanics and mapped Taputapu Volcanics were also collected and analyzed in order to confirm differences between the Leone and Taputapu Volcanics in the existing surface sample data and to compare to the Leone and Taputapu Volcanics in the core. These surface sample locations are displayed in Figure 5.

Major and minor elements were analyzed and reported as oxides in dry weight percent. Major element abundances are presented below in Table 4. Minor element abundances as well as laboratory reports can be found in GEOLOGICA (2016c). The results indicate that the samples are very similar with silica (SiO_2) ranging from 42.0 to 49.4 dry weight %, calcium oxide (CaO) from 1.7 to 3.9 dry weight %, and aluminum oxide (Al_2O_3) from 10.6 to 15.8 dry weight %. The greatest variation appears to be in magnesium oxide (MgO) which varies from 3.6 to 14.8 dry weight %.

Table 4. Major element abundances from core and surface samples, reported as dry weight percent.

Laboratory	Sample Location	Depth (ft)	SiO_2	TiO_2	Al_2O_3	Fe_2O_3	MnO	MgO	CaO	Na_2O	K_2O	LOI	SUM
			Dry Weight %										
GNS	TGH-1	87	45.26	5.17	14.37	15.04	0.16	6.50	8.87	3.03	1.13	-0.38	99.16
	TGH-1	387	48.27	3.70	14.07	13.05	0.15	6.16	8.27	3.19	1.44	0.68	98.98
	TGH-1	494	48.16	3.92	14.17	13.25	0.14	6.57	8.17	3.32	1.47	-0.30	98.88
	TGH-1	696	43.63	3.42	10.59	13.97	0.16	13.64	10.23	1.68	1.21	0.52	99.05
	TGH-3	162	43.67	3.40	10.92	13.91	0.17	13.21	10.60	2.62	1.10	-0.61	99.00
	TGH-3	505	40.17	4.60	11.65	15.44	0.17	12.64	10.24	1.57	0.82	1.59	98.89
	TGH-3	618	49.37	3.06	15.56	12.64	0.15	3.63	7.36	3.92	1.90	0.76	98.35
	TGH-3	703	46.93	3.92	15.14	14.54	0.14	5.11	7.64	3.48	1.41	0.60	98.91
	Ili'ili-01	Surface	43.82	3.15	10.88	13.80	0.16	13.60	10.56	2.07	1.12	-0.05	99.10
	Turtle&Shark–01	Surface	40.35	3.19	10.29	12.87	0.15	14.80	9.68	2.48	1.01	4.08	98.92
	Amaluia-01	Surface	46.42	3.88	15.77	15.18	0.19	4.64	6.84	3.06	1.41	1.58	98.96
UH	TGH-3	254	44.79	3.64	12.27	13.60	0.17	11.01	9.93	1.45	2.04	9.18	99.33
	TGH-3	307	44.11	3.80	10.74	13.28	0.18	13.38	10.07	3.04	0.74	0.00	99.40
	TGH-3	492	42.41	4.52	12.28	14.34	0.17	12.21	10.27	1.93	1.26	1.88	99.19
	TGH-3	503	41.97	4.65	12.44	14.56	0.18	12.32	10.17	2.01	0.89	2.83	98.74
	TGH-3	1146	46.47	4.36	14.62	13.39	0.16	6.92	9.24	3.11	0.48	1.83	0.00

GNS = GNS Science, Taupo, New Zealand

UH = University of Hawaii

5.4.2. Thin Section Petrography

Five thin sections were made and analyzed from core in each of the two TGHs in order to describe the major rock forming minerals, textures and alteration mineralogy of the rocks. The thin section analysis focused on evidence of hydrothermal alteration. Samples were selected which had significant secondary mineralization which could be observed microscopically.

Thin section petrographic analysis was largely consistent with observations made from core logging. Generally weak alteration of the lavas observed in the initial core logging was confirmed by this analysis (Figure 13); however, the morphologies of alteration minerals such as thin, acicular, radiating zeolites at 2,097 ft bgs were more clearly imaged (Figure 13).

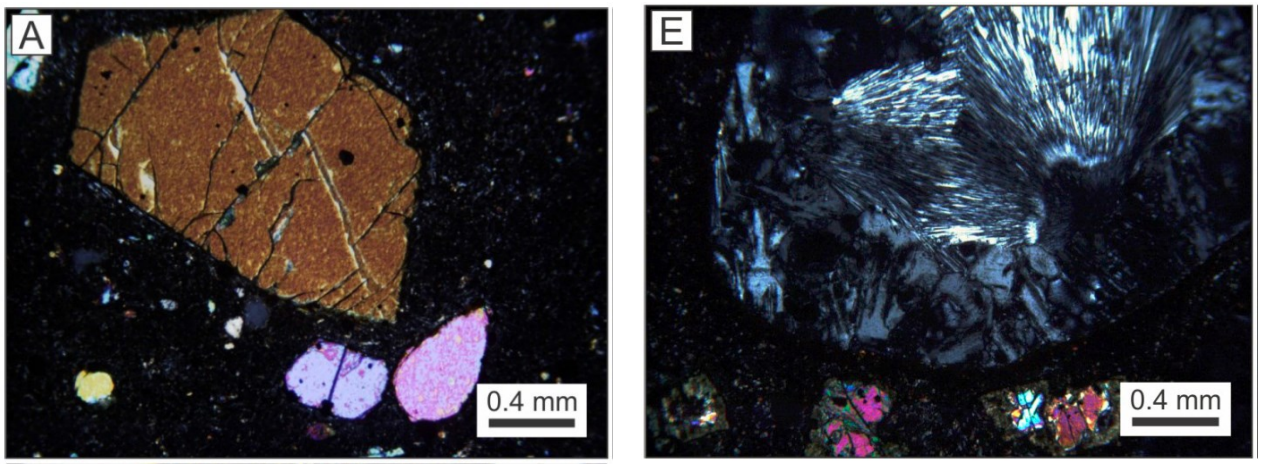

Figure 13. Photomicrographs of thin sections from cores. (A) Orthopyroxene phenocrysts in microcrystalline groundmass in seriate porphyritic basalt from TGH-1 at 1,950 ft bgs. (E) Vesicles filled with radiating zeolite crystals in basaltic scoria from TGH-3 at 2,097 ft bgs, as viewed in thin section under cross-polarized light.

5.4.3. Short-wave Infrared (SWIR) Spectroscopy

Although TGH-3 was closer to the HRZ rift axis and could be expected to have higher temperature alteration mineralogy than TGH-1, no consistent succession of alteration clay mineralogy indicative of a geothermal system was observed in the core logging of either hole. In order to evaluate the clay alteration mineralogy in more detail, 33 samples from TGH-3 from 242 ft to 2101 ft bgs were analyzed with Short-wave Infrared (SWIR) Spectroscopy.

Results indicate that while there is a slight trend toward higher-grade clay alteration from possible kaolinite beginning at 532 ft bgs to smectite at 590 ft bgs to possible mixed-layer illite-smectite at 837 ft bgs, the spectra are very noisy, aspectral, and/or weak. Below 1,853 ft bgs no clays were detected in the samples analyzed.

5.4.4. X-ray Diffraction

Three samples with potentially interesting carbonate and zeolite mineral morphologies from within the low-resistivity zone were selected for clay-separate X-ray diffraction (XRD). These samples were from TGH-1 at a depth of 1,804 ft bgs and from TGH-3 at depths of 1,100 ft and 2,100 ft bgs.

Non-geothermal related clays such as chabazite and thomsonite were detected in TGH-1 at 1,804 ft bgs. Potentially hydrothermal-related clays such as illite and aragonite were detected in the TGH-3 sample from 1,100 ft bgs as well as the zeolites gmelinite, natrolite, and gonnardite in the TGH-3 sample from 2,100 ft bgs. The diffraction peaks for all of these samples were diffuse and of low intensity, indicating relatively little clay overall.

Additionally, two samples from TGH-1 at 1,380 ft and 1,491 ft bgs, which had inconclusive clay mineralogy results reported from the SWIR analysis, were crushed and had both their air-dried and glycolated clay separately analyzed by XRD. Trace smectite and minor quantities of illite were detected in the TGH-1 sample from 1,380 ft bgs, indicating generally low temperatures. Trace kaolinite and minor quantities of smectite were detected in the TGH-1 sample from 1,491 ft bgs, also indicating generally low temperatures.

5.4.5. Carbon-14 Age Dating

The age-dated carbonate samples are from the upper carbonate unit (dominantly reef-forming corals) at depths of 274.25 ft, 295.5 ft, and 298 ft bgs, and from the lower carbonate unit (dominantly marl) at 453 ft bgs (Reinhard, 2016). Sample data are presented below in Table 5.

Median ages for the upper carbonate unit are progressively older with depth, from 4,438 years before present (B.P.) for the shallowest sample (274.25 ft) to 7,128 years B.P. at the unit's base (298 ft). The deepest carbonate sample (453 ft), from the lower marly unit, has an age of 10,385 years B.P.

Table 5. Carbon-14 age dates for carbonate samples selected from TGH-3 core. Work performed by University of California, Riverside at the Keck Carbon Cycle AMS Facility, UC, Irvine (Reinhard, 2016).

UCIAMS #	Sample Name	Depth (feet bgs)	Material	Conventional Age (years B.P.)	Calibrated Median Age (years B.P.)	2 Standard Deviation error	
						Min (years B.P.)	Max (years B.P.)
169364	3-274.25	274.25	Unidentified Shell	4365 ± 20	4,438	4,336	4,529
169365	3-295.5	295.5	Unidentified Coral	6550 ± 20	6,997	6,899	7,122
169367	3-298	298	Unidentified Shell	6655 ± 20	7,128	7,014	7,220
169366	3-453	453	Unidentified Coral	9585 ± 25	10,385	10,254	10,497

B.P. = Before Present

Radiocarbon concentrations are given as fractions of the Modern standard, $D^{14}C$, and conventional radiocarbon age, following the conventions of Stuiver and Polach (1977).

Sample preparation backgrounds have been subtracted, based on measurements of 14C-free wood (organics) and calcite (carbonates). The radio-carbon ages were calibrated using the Calib program (http://calib.qub.ac.uk/calib/). For calibration a ΔR value of 57 ± 23 (Phelan, 1999) and the Marine13 calibration curve were used.

All results have been corrected for isotopic fractionation according to the conventions of Stuiver and Polach (1977), with $d^{13}C$ values measured on prepared graphite using the AMS spectrometer. These can differ from d13C of the original material, if fractionation occurred during sample graphitization or the AMS measurement, and are not shown.

5.5. Temperature Logging

During drilling, bottom-hole temperature (BHT) measurements were collected using a HOBO U12-015 or HOBO U12-015-02 temperature logger installed at the bottom of the coring string. Timing of BHT collection with relation to timing of drilling fluid circulation varied, which subsequently influenced the resulting temperature measurements. In addition, multiple heat-up temperature surveys were conducted on TGH-1 and TGH-3 after completion of drilling using a modified deep sea fishing rod and electric reel with digital depth counter and graduated line. Combined temperature-depth logs for TGH-1 and TGH-3 are included in Figure 14 and Figure 15.

5.5.1. Temperature Gradient Data

TGH-1

Immediately after completion of TGH-1, two End of Well (EOW) temperature surveys were conducted ~12 hrs apart on 11 October 2015 with the rig still on the hole. After release of the rig, six additional logs were conducted in TGH-1 between 28 October and 30 November 2015. The logs show relatively consistent temperature profiles with no significant heating or cooling zones over time within the well (Figure 14).

Multiple surveys of TGH-1 confirm that below the unconfined shallow aquifer the temperature gradient is conductive and ~20-30°C/km. The bottom hole temperature is ~37°C.

TGH-3

Immediately after completion of TGH-3, two EOW temperature surveys were conducted ~12 hrs apart on 16 November 2015 with the rig still on the hole. Five additional logs were completed in TGH-3 between 18 November and 07 December 2015, with a final log on 13 January 2016. The logs show relatively consistent temperature profiles except at ~905 ft bgs (Figure 15) where a rubble zone was encountered, causing borehole washout and requiring two cement jobs. This zone was apparently heated by large volumes of drilling water and/or heat of hydration from the cement curing process. Repeat surveys show this transient heat dissipating.

Multiple surveys of TGH-3 confirm that below ~-900 ft msl, the temperature gradient is conductive and ~20-30°C/km. The bottom hole temperature is ~37°C.

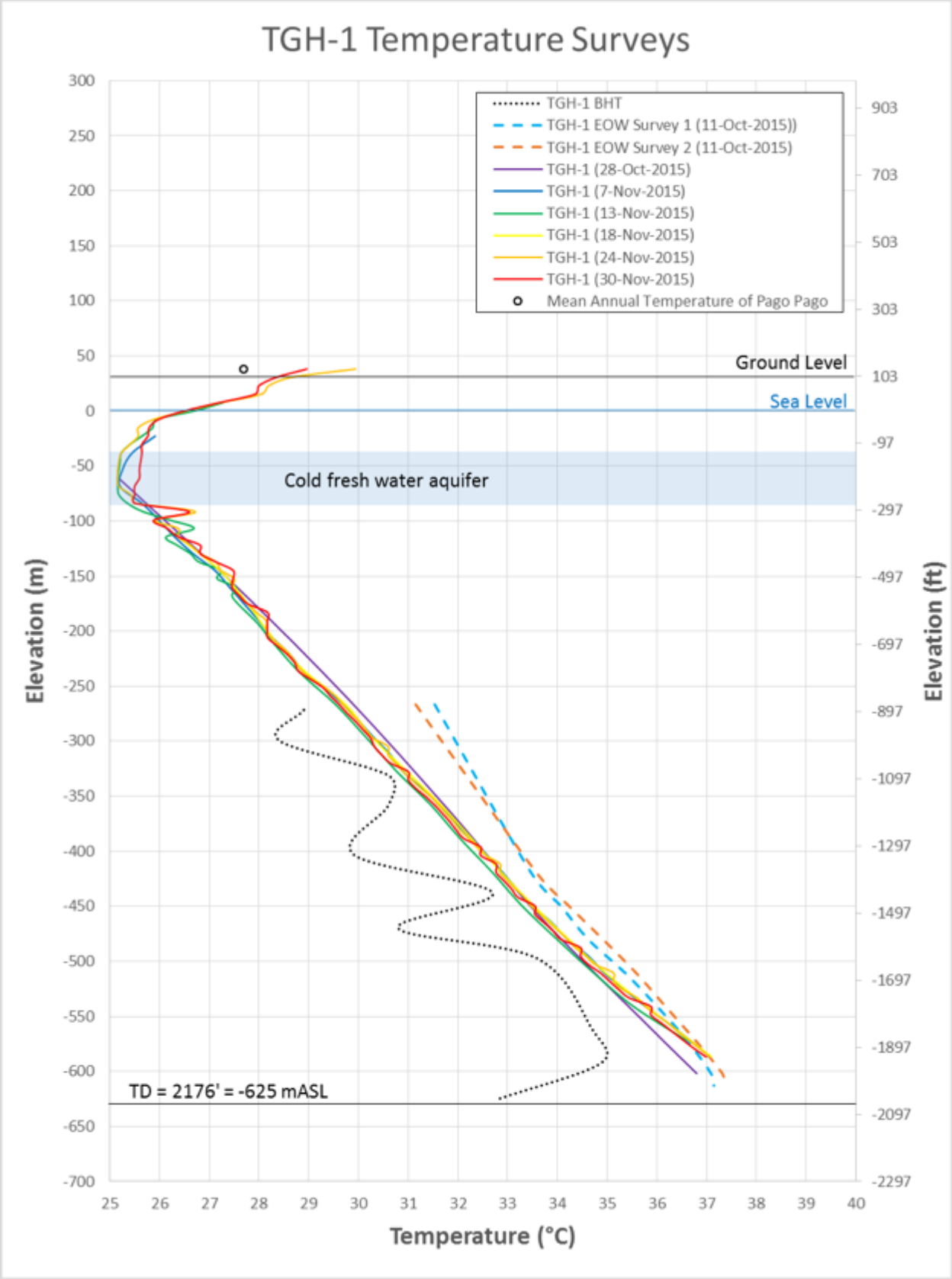

Figure 14. Combined temperature logs for TGH-1. The BHT survey presents a series of bottom hole temperatures collected with maximum recording thermometers during drilling. All other surveys were collected using the HOBO tool.

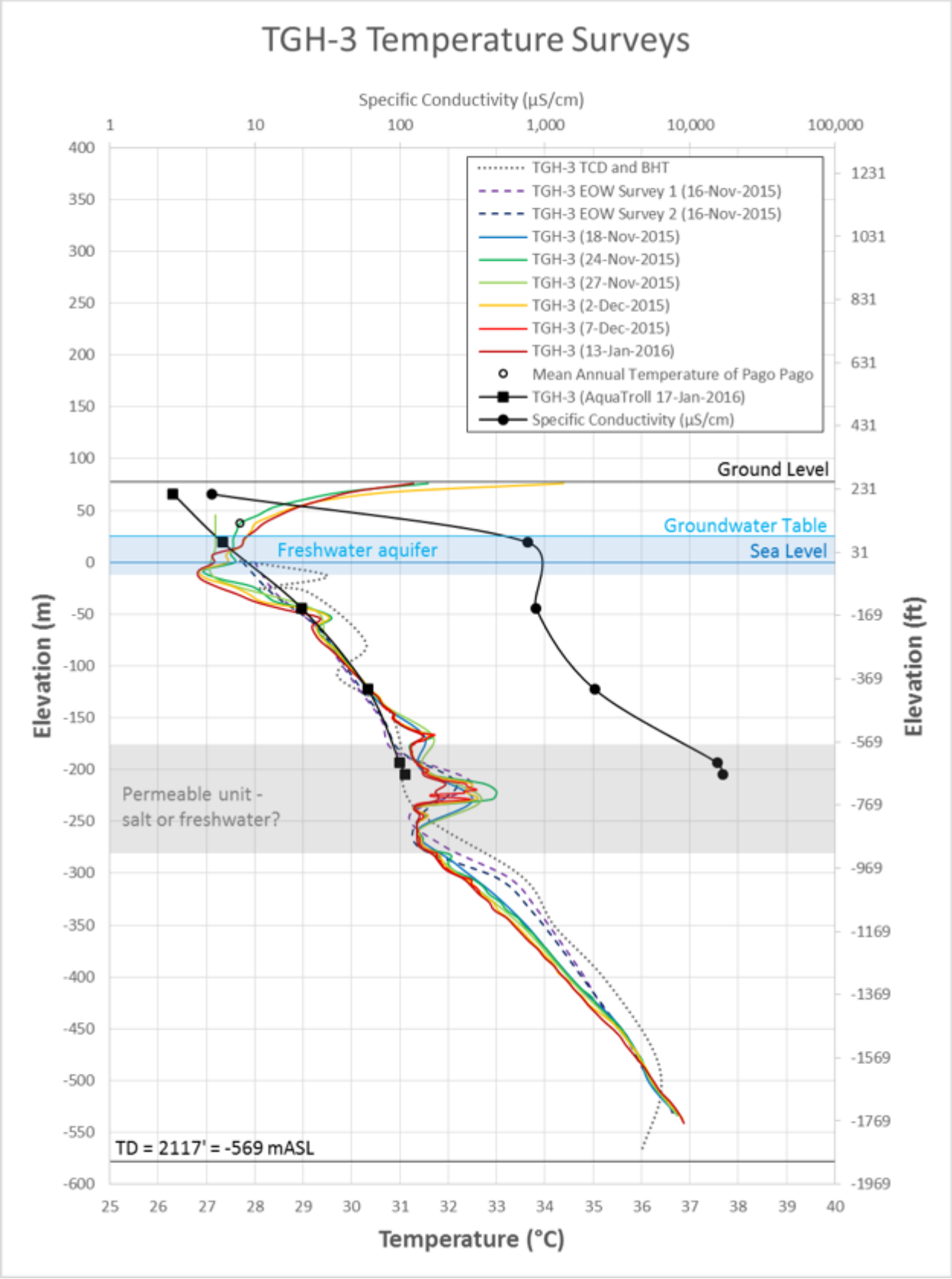

Figure 15. Combined temperature and conductivity logs for TGH-3. The BHT series presents a series of bottom hole temperatures collected with maximum recording thermometers during drilling. All other surveys were collected using the HOBO tool.

5.6. Hydrogeological Data

An important aspect of the data collection program was measuring the depth of any groundwater aquifers. An Aqua TROLL 200 temperature/depth/salinity (TDC) sonde was deployed approximately every shift change during drilling in an attempt to measure temperature changes, which might suggest the presence of hydrothermal fluids (GEOLOGICA, 2015). In addition, the sonde measurements were intended to identify the first brackish (saline) water and thus the bottom of the freshwater lens assumed to be sitting on top of seawater.

TGH-1

Static groundwater in TGH-1 was measured at ~130 ft bgs, approximately -5 feet msl; however, analysis of the static temperature logs indicates that static ground water may be higher at ~80 ft msl. A freshwater aquifer was encountered from 130 to ~400 ft bgs (-5 to ~-275 ft msl). The freshwater/saltwater interface appears to occur between approximately 355 to 620 ft bgs (-230 to -495 ft msl). The sonde was deployed at 355 ft bgs (-230 ft msl) and indicated fresh water. The interval from 292 to 402 ft bgs (-167 to -277 ft msl) was drilled without returns. When the TDC sonde was deployed at 620 ft bgs (-495 ft msl), it indicated saltwater. Equilibrated temperature surveys indicate that the freshwater aquifer may extend as deep as 425 ft bgs (-300 ft msl).

TGH-3

Static groundwater in TGH-3 appears to be at ~150 ft bgs, approximately 102 ft msl. A freshwater aquifer was encountered from ~150 to 350 ft bgs (102 to -98 ft msl). The freshwater/saltwater interface appears to occur at ~350 ft bgs (-98 ft msl). The TDC sonde was deployed at 344 ft bgs (-92 ft msl) and indicated fresh water. When the sonde was deployed at 382 ft bgs (-130 ft msl), it recorded a significantly elevated conductivity indicative of brackish water. Equilibrated temperature surveys indicate that the primary freshwater aquifer may extend as deep as 350 ft bgs (-98 ft msl) with a deep aquifer from ~850 to 1,150 ft bgs (-598 to -898 ft msl). It is currently unknown whether the deep aquifer is freshwater or saline.

Subsequent to the removal of BQ rods, ASPA performed a downhole TDC survey on 17 January 2016 to a depth of ~920 ft bgs (-668 ft msl) in the open hole. The salinity values, measured in specific conductivity units, from this survey are plotted on Figure 15. The specific conductivity increases with depth, but the highest reading is ~16,000 µS/cm whereas drinking water is typically 0.05-500 µS/cm and seawater is typically ~50,000 µS/cm. Therefore, it appears the borehole is still significantly influenced by drilling fluid (primarily fresh surface water) and/or intra-wellbore mixing of fresh and saltwater aquifers. Discrete zones may have been flushed by seawater, but the precision of the survey is not high enough to investigate this possibility. Any further salinity surveys of TGH-3 would require purging of drilling fluid and time to re-equilibrate in order to be representative of the natural state fluid column.

5.7. Surface Field Geology

In the course of the geothermal investigation, GEOLOGICA selectively confirmed and re-mapped geology in the area of the HRZ with both field mapping and remote sensing methods. Source maps consulted in this process included Stearns (1944), NPS (2008), and Izuka et al. (2007). Confirmation of the geomorphology and structure of the HRZ was made during Phase 2 using high-resolution LiDAR topographic imagery resulting in mapping of numerous lineaments and inferred faults. The LiDAR and structural mapping, previously reported in GEOLOGICA (2014a) indicated the presence of near-vertical fractures and lineaments.

During Phase 3, strikes and dips of bedding in Leone Volcanics were measured in the field at several locations on the Tafuna-Leone Plain.

Two surface samples of mapped Leone Volcanic basaltic lavas and one sample of mapped Taputapu Volcanic basaltic lava were collected in the field for XRF analysis as described above. Location data are tabulated in Table 3 and major element abundances are tabulated in Table 4.

Morphological analysis, using LiDAR, of two youthful-looking craters mapped as Taputapu Volcanics west of Olotele Crater resulted in these features being remapped as Leone Volcanic cinder cones.

6. ANALYSIS

6.1. Drilled Lithology and Stratigraphy

While the lithology of the cuttings and core represent observations made during logging and drilling, assignment of the lithology to specific stratigraphy or formations involves analysis and interpretation. Lithologies present in the two TGHs are similar, except at shallow depths (<1,000 ft bgs). The Leone Volcanics are thinner at TGH-1 than at TGH-3 (~100 ft vs ~500 ft) and are covered by ~100 ft of Taputapu Volcanics-derived sediments.

6.2. Leone Carbonate Units and Implications for Tutuila Subsidence Rate

The Leone Carbonates are obvious in the TGH-3 core, appearing first in the form of a coral reef and slightly deeper as marly sediments. Carbonates were not observed in TGH-1; however, they may have been encountered in the zone of total lost circulation from 292 ft to 376 ft bgs.

The radio-carbon age dates for the TGH-3 carbonates indicate two periods of deposition from ~4,000-7,000 years B.P. for the coral reef and at ~10,000 years B.P. for the marly sediments. Accumulation of the reef carbonates required a depositional environment within the photic zone which both 1) was subsea, but not too deep (<100 ft below sea level, -30 masl), and 2) did not receive volcanic deposits.

Leone Volcanism may have either been inactive during these periods or did not deposit volcanic material at this location because 1) the eruptions were dominantly non-pyroclastic lavas that flowed elsewhere, and/or 2) ash falls or other airborne deposits were blown elsewhere.

The stratigraphically deeper and older marly unit was deposited in deeper water ~10,000 years B.P., probably shoreward of an active reef in a lagoon. These fine-grained sediments with relatively small shell fraction represent reef materials eroded off the active reef and deposited in the adjacent deeper water. As the Leone Volcanic lava flows continued to fill the lagoon on top of the marly layer, the water became shallow enough (<100 ft, <30 m) to support an active reef beginning ~7,000 years B.P. Eventually, at the TGH-3 location, Leone ash deposits and lava flows completely covered the reef and built the Tafuna-Leone Plain up above sea level ~4,000 years B.P.

This range of dates defines a period of rejuvenated volcanism of Tutuila. Since Leone Volcanics underlie the marly clay unit and overlie the reef unit, the oldest Leone Volcanics are >10,000 years B.P. and the youngest Leone Volcanics erupted <4,000 years B.P. The latter dates are consistent with dates from charcoal found between lava flows and overlying ash deposits in the uppermost Leone Volcanics of 1,000 to 1,600 years B.P. (Addison et al., 2005). The date for the initiation of Leone Volcanism is unbounded by this data and therefore Leone Volcanism may have begun pre-Holocene (~11,700 years B.P.).

Global sea levels have been relatively stable over the last 7,000 years, with estimates of sea level change generally ranging from less than a ~10 m rise (Pirazzoli, 1991) since 7,000 years ago, to up to a 3 m drop from the Holocene High Stand in the equatorial Pacific Ocean ~5,000 to ~1,500 years ago (Grossman et al., 1998). All of the reef carbonate samples from the upper carbonate unit in TGH-3 were collected from core at depths currently below sea level. Assuming that these shells and corals were at or just below sea level when they formed, we can calculate the estimated subsidence rate of Tutuila between ~7,000 years B.P. and the present day.

The minimum and maximum subsidence rates for the reef samples implied by their Carbon-14 ages are tabulated in Table 6. The subsidence rates range from -0.74 mm/yr (assuming a 10 m rise in sea level) to 2.4 mm/yr (assuming a 3 m drop in sea level) with a range of 1.5 to 2.0 mm/yr if constant sea level is assumed over the last ~7,000 years. These subsidence rates are consistent with the estimate of 1.1 to 1.4 mm/yr calculated by Dickinson (2007) for Upolu and the estimate of 1.0 to 1.2 mm/yr calculated by Sand et al. (2016) for Manono Island, just off the west coast of Upolu.

A more detailed Holocene sea level history of Tutuila would allow for more precise estimates of subsidence rates.

Table 6. Calculated subsidence rates for upper carbonate samples in TGH-3.

UCIAMS #	Reef Sample Elevation (masl)	Calibrated Age (years B.P.)			Subsidence Rate Constant Sea Level (mm/yr)		Subsidence Rate 10 m Rise in Sea Level (mm/yr)		Subsidence Rate 3 m Drop in Sea Level (mm/yr)	
		Median	2 Standard Deviation error							
			Min	Max	Min	Max	Min	Max	Min	Max
169364	-6.8	4,438	4,336	4,529	1.56	1.50	-0.74	-0.71	2.26	2.16
169365	-13.3	6,997	6,899	7,122	1.92	1.86	0.47	0.46	2.36	2.28
169367	-14.0	7,128	7,014	7,220	2.00	1.94	0.57	0.56	2.43	2.36

B.P. = Before Present

Subsidence Rate, Constant Sea Level {Min, Max} calculated as (Reef Sample Elevation) ÷ (Calibrated Age {Min, Max}) *1000.

Subsidence Rate, 10 m Rise in Sea Level {Min, Max} calculated as (Reef Sample Elevation + 10) ÷ (Calibrated Age {Min, Max}) *1000.

Subsidence Rate, 3 m Drop in Sea Level {Min, Max} calculated as (Reef Sample Elevation - 3) ÷ (Calibrated Age {Min, Max}) *1000.

6.3. Identifying the Leone-Taputapu Contact with major element ratios

The young Holocene-age Leone Volcanics are difficult to distinguish visually from the older Pleistocene-age Taputapu Volcanics in both outcrop and core. Both appear as relatively unaltered basaltic lava flows interlayered with altered tuffs and volcaniclastic sediments. Total alkali ($Na_2O + K_2O$ in weight %) and silica (SiO_2 in weight %) in laboratory analyses of whole rock samples were used to distinguish the two units as detailed below and as described previously (e.g. Hawkins and Natland, 1975; Natland, 1980; Natland and Turner, 1985; and Konter and Jackson, 2011).

Specifically, the Total Alkali-Silica (TAS) diagram (Figure 16) is used to discriminate volcanic rock types by comparing SiO_2 (weight %) versus $Na_2O + K_2O$ (weight %) for various volcanic rocks. Samples from Holocene post-erosional Leone Volcanics from the surface and TGH-3 are slightly more mafic (lower silica) with higher sodium and potassium than the older Taputapu Pleistocene shield-building Volcanics from the surface and TGH-1 samples. Both Leone and Taputapu Volcanics have compositions from basanites and basalts, to trachy-basalts, but Leone Volcanics include foidites.

When compared to fields on a TAS diagram (Figure 16) defined by previously reported silica and alkali results from both Leone and Taputapu Volcanics (e.g. Eyre and Walker, 1991) and recent data from University of Hawaii (Paul Eyre, 2016), TGH-1 and TGH-3 results mostly confirm the previous formation chemical distinctions, albeit with a somewhat more continuous range. For example, despite having been collected from an area mapped as Leone Volcanics, the surface sample from Ili'ili on the edge of the TGH-3 drilling pad, sample #15 in Figure 17 does not plot within the previously identified range for Leone Volcanics. In addition, core samples #12 and #21 (both from TGH-3), and surface sample #16 plot outside the field for Leone Volcanics, but not within the range of Taputapu Volcanics. Some of this scatter may be due to weathering state of the samples and other alteration processes, which occurred post-deposition.

The sample from TGH-3 at 505 ft bgs (#12) analyzed by GNS plots very close to the sample from TGH-3 at 503 ft bgs (#21) analyzed by UH. This section of core was logged as marly carbonate overlying the Taputapu Volcanics. These TGH-3 marly carbonates and a sample from Malaeimi Well 110 at 112 ft bgs (#5), which was tentatively identified as Leone Volcanics by Eyre and Walker (1991), are outliers with the lowest SiO_2 of any of the reported Tutuila rock chemistries. The surface sample from the Turtle and Shark Hotel (#16) exhibits the distinctive low-silica chemistry associated with Leone Volcanics identified by Natland and Turner (1985), but also has lower alkalis, demonstrating that the range for Leone Volcanics is larger than previously reported.

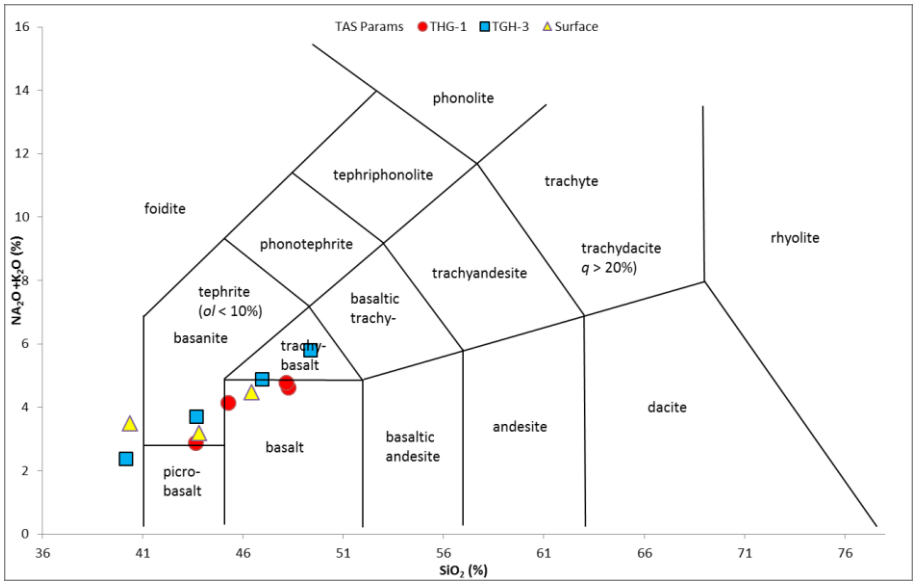

Figure 16. Total Alkali vs Silica Diagram of Tutuila basalt samples showing rock types. Petrologically, Leone and Taputapu Volcanics have compositions spanning foidites through basanites and basalts, to trachy-basalts.

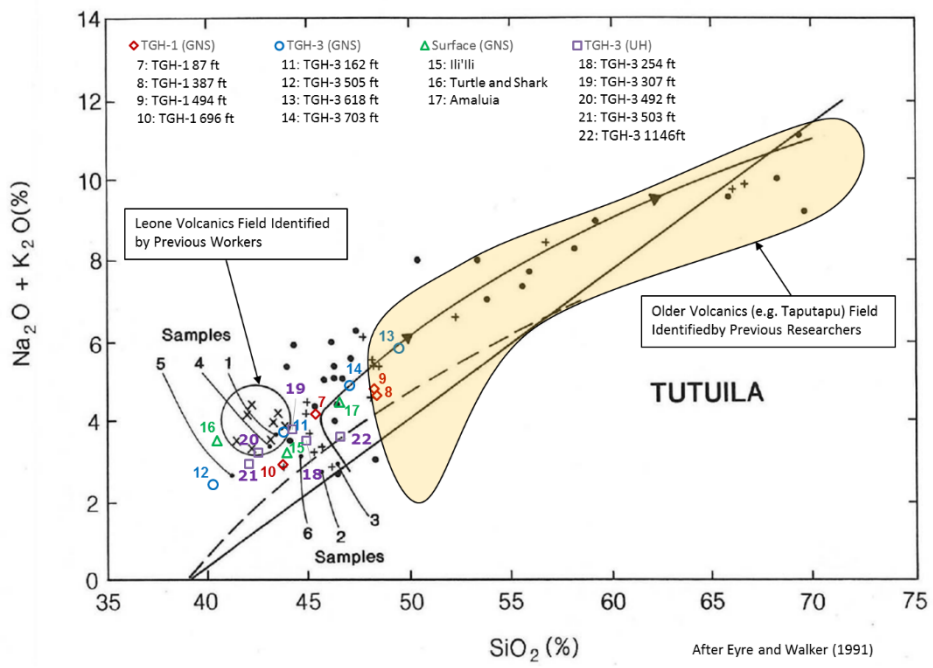

Figure 17. Total Alkali vs Silica Diagram of Tutuila basalt samples *after* Eyre and Walker (1991) which itself is *after* Natland (1980) and Hawkins and Natland (1975). Samples analyzed by GNS from the present study are numbered 7-17 and samples analyzed by UH are numbered 18-22. All listed depths are in ft bgs.

Plots of silica, calcium (as CaO), and zircon vs magnesium (as MgO), as in Figure 18 to Figure 20 (after Eyre, 2016), indicate a clearer distinction between the basalts of Leone and Taputapu Volcanics. In TGH-1 the shallowest sample from 87 ft bgs is clearly in the Taputapu Volcanics trend. Rather than an in-place lava flow, this core is interpreted to be erosional material from Taputapu Volcanics, possibly a boulder, deposited from the highland above the base of the cliff just north of TGH-1. This section was originally logged as

lava flow based on cuttings because this interval was drilled, not cored. Distinguishing between boulders and in-place lava flows in cuttings is very difficult. Therefore, this section is classified as Taputapu Volcanic alluvium. The next deeper sample from TGH-1 at 387 ft bgs also plots well within the Taputapu Volcanic range and is obviously in-place lava flow based on visual core analysis.

The shallowest TGH-3 sample (162 ft bgs, #11) plots within the Leone Volcanic range. The second shallowest TGH-3 sample (505 ft bgs, #12) plots outside of the Leone Volcanic range as a marly carbonate. Both these samples are relatively primitive (low SiO_2, high MgO, Ni, and Cr) and, more importantly, plot outside the Taputapu Volcanic group. The next deeper sample from TGH-3 at 618 ft bgs plots within the Taputapu Volcanic group, indicating the contact is between 505 ft and 618 ft bgs.

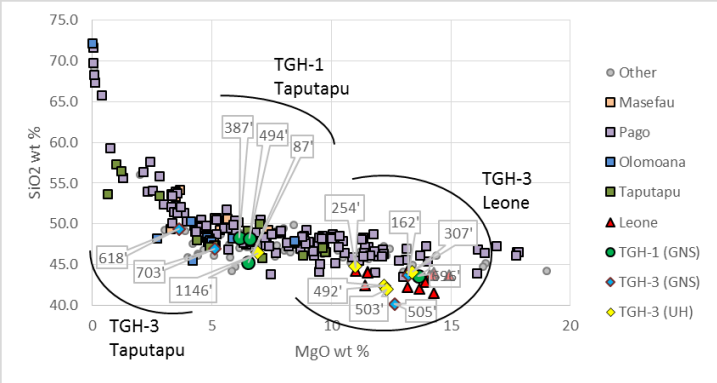

Figure 18. SiO2 vs MgO plot of Tutuila basalts, after Eyre (2016).

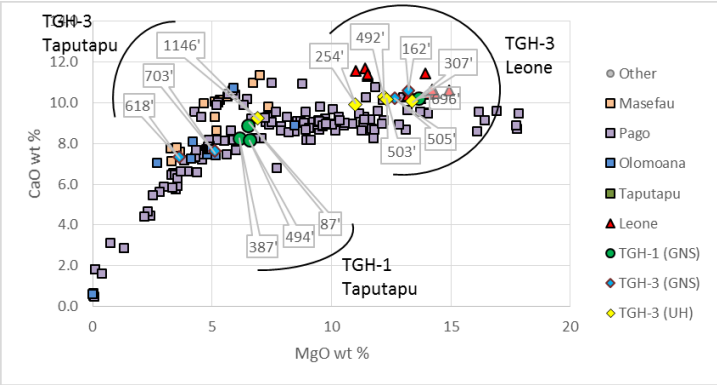

Figure 19. CaO vs MgO plot of Tutuila basalts, after Eyre (2016).

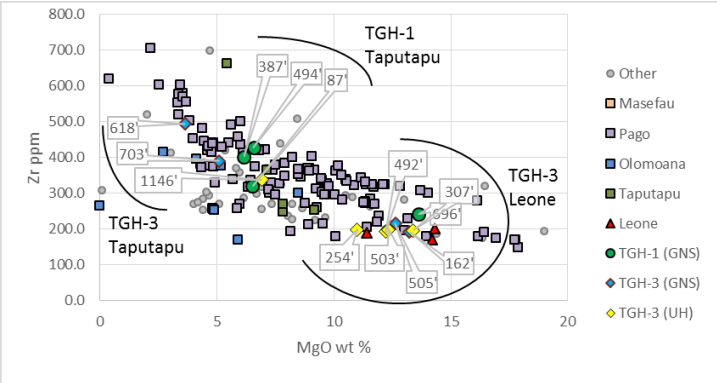

Figure 20. Zr vs MgO plot of Tutuila basalts, after Eyre (2016).

The chemical distinctions between Leone and Taputapu Volcanics suggest that the youngest volcanics (Leone) represent magmas that were derived deeper in the mantle and reached the surface with limited residence time in the crust. Such magmas commonly erupt via dikes that propagate along relatively narrow vertical fractures (<100 m width) perpendicular to the local minimum stress. The whole rock chemistry indicates that there is no reason to expect significant shallow magma residence during the latest episode of volcanism, and thus there may be no shallow and long-lived magma source associated with the HRZ to generate a geothermal system.

6.4. Structure

The HRZ has been described by previous workers (e.g. Stearns, 1944; Natland, 1980) as a rift – a structural setting with extensional strain. Leone Volcanics are assumed to have erupted along a plane of weakness in the existing crust, possibly associated with the tearing of the Pacific Plate at the Tonga Trench ~100 km to the south (Keating, 1992). GEOLOGICA mapped lineaments in the HRZ during Phases 1 and 2 (GEOLOGICA, 2014b), some of which were classified as faults (Figure 5); however, no displacements have been observed on mapped faults in the HRZ.

High-angle fractures and faults observed in core in both TGHs are likely related to the structure of the HRZ and indicate a normal faulting regime. Since the core is not oriented, there is no way to determine the dip direction of the fractures, but high-angle and dip-slip slickensides observed in both core indicate extensional normal faulting. This is the only direct evidence from either mapped geology or borehole geology of the extensional stress regime of the HRZ and represents an important new finding of the investigation.

Fractures in the more brittle lithologies, such as flows and indurated tuffs of both TGHs, are variably open and vein-filled, indicating multiple episodes of fracturing and/or multiple fluid circulation regimes. The fluid circulating within the fractures was not hydrothermal, based on the low-temperature mineralogy of the veins.

Though primary porosity of the lavas, as with most of the fine-grained and clay-rich volcaniclastics, is very low, there is abundant secondary permeability. This secondary permeability is related to fracturing of brittle lava flows and brecciated volcaniclastics forming horizontal permeability. The stratigraphic nature of the fractured brittle layers confines this horizontal permeability to discrete horizons, which are terminated abruptly in the vertical direction by low-permeability clay-rich volcaniclastics consisting of devitrified lapilli tuff, ash and debris flows, as illustrated in a volcanic landscape block model in Figure 21 (Keating, 1992). In some places, these fractured volcanics may be laterally extensive enough to constitute an aquifer (thick, well-jointed lava flows, for example). Furthermore, the deeper laterally permeable zones may provide confined aquifers except where connected by high-angle dikes, faults and fractures in the HRZ-related system.

The pillow lavas and highly fractured hyaloclastites associated with the emergent phase of island volcanos are not observed in the Taputapu intervals of either THG.

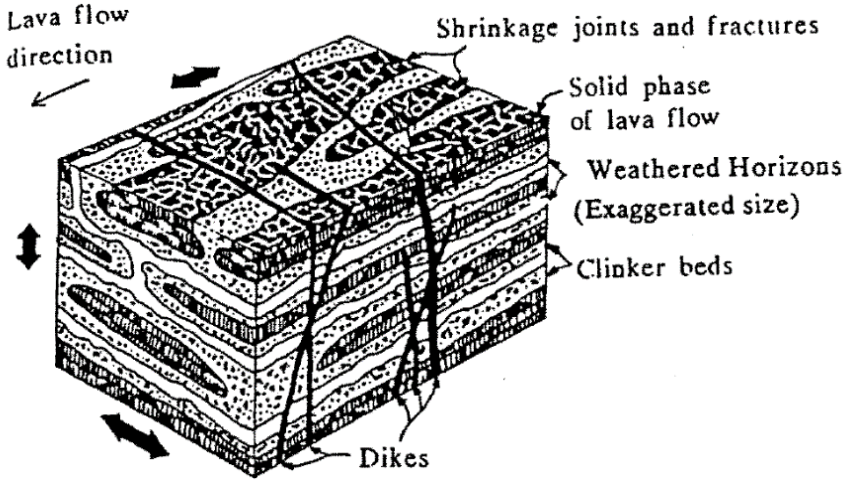

Figure 21. Block diagram illustrating the complex relationship of lava flow units and volcaniclastic units in volcanic landscapes. Dikes can further complicate the hydrology by acting as either vertical barriers or permeable conducts for fluid movement. Figure reproduced from Keating (1992).

The lava flows of Leone Volcanics generally form shallow-dipping (<10-20°) flatlands, sloping toward the sea. Surface measurements of flow orientations confirmed these strikes and dips along the southern coast in Leone Volcanics.

The Holocene Rift Zone bisects the Tafuna-Leone Plain and rises in a ridge ~100 m above the plain and striking ~SSE from Olotele Crater in the north where it is less than a mile wide to Fagatele and Fogama'a Craters in the south where the rift zone widens to ~2 miles. Thick vegetation obscures the structure of the HRZ, however LiDAR interpretation has allowed tentative identification of NNW to SSE trending lineaments, which may be normal faults. Vertical fractures in both TGHs and apparent faults with dip-slip slickensides appear to confirm this interpretation. These faults are presumably normal and indicative of an extensional stress regime within the HRZ, conducive to forming and maintaining vertical permeability. Although there is no apparent hydrothermal fluid within the HRZ, this structural interpretation is consistent with the conceptual model from Phase 2.

Two young-looking craters west of Olotele Crater, including Oloava crater, (Figure 5) were previously mapped as Taputapu Volcanics by Stearns (1944), but are more likely Leone Volcanics and have been remapped as Leone Formation cinder cones on the inset map in

Figure 5. This reclassification suggests that understanding the geology of Tutuila may benefit from thorough island-wide remapping of geology leveraging modern remote sensing techniques.

6.5. Alteration

Most of the mineral alteration identified during core logging, and in the SWIR, petrographic thin section and the XRD analysis is producible by low-temperature processes such as tropical weathering, burial diagenesis and interaction with saltwater. Other minor elevated-temperature alteration such as trace illite in TGH-1 and TGH-3 might have occurred during initial high-temperature interaction with surface waters immediately after the erupting lavas crystalized, or during short-lived pulses of heat such as dike emplacement. None of the samples analyzed indicate the pervasive, long-lasting, high-temperature alteration characteristic of a geothermal system.

6.6. Temperature Gradients and Hydrogeology

TGH-1

Multiple surveys of TGH-1 confirm that below the unconfined shallow aquifer, the temperature gradient is conductive. The linear gradient is ~20-30°C/km, consistent with the worldwide continental average, and somewhat less than typical oceanic crust gradients of ~45°C/km (Long et al., 2009). The bottom hole temperature is ~37°C.

The cold (compared to the average surface temperature) fresh water aquifer is readily apparent in the temperature profile and extends from ~-35 ft msl to -295 ft msl – a total thickness of ~260 ft. No other deeper aquifers are apparent.

TGH-3

Multiple surveys of TGH-3 confirm that below ~-1000 ft msl the temperature gradient is conductive and ~20-30°C/km, consistent with TGH-1. The bottom hole temperature is ~37°C, identical to TGH-1.

The cold fresh-water aquifer is readily apparent in the temperature profile and extends from ~+80 to -15 ft msl – a total thickness of ~100 ft. Interestingly, a second deeper aquifer appears to exist from ~-575 to -900 ft msl. Although some limited salinity measurements were recorded to this depth, it is not clear if these are representative due to mixing effects within the wellbore. Further hydrogeological investigations may find this aquifer to be fresh water. If this is confirmed by future studies, this aquifer may represent a new groundwater resource for Tutuila.

The gradients measured in TGH-1 and TGH-3 are low given the location of Tutuila over thin oceanic crust and the proximity of TGH-1 to the rejuvenated volcanism of Leone Volcanics and the Holocene Rift Zone. The low temperatures reflect the absence of heat anomalies and suggest that the heat generated by the Leone Volcanic magmas has dissipated. The gradients are somewhat lower than expected for a young volcanic province, with or without a geothermal system, and may be explained by:

1) Lack of significant magma storage or intrusion in the shallow crust;

2) The great thickness of Pleistocene and older shield volcano basalts (>3000 m) mounded on the seafloor and forming the bulk of Tutuila, and insulating Tutuila from the heat of the upper mantle; and/or

3) Proximity to the deep and cold abyssal plains of the Pacific Ocean (just above 0°C) only several kilometers offshore.

7. INTEGRATION OF PHASE 3 RESULTS WITH PREVIOUS EXPLORATION RESULTS

In order to update the geothermal conceptual model and assessment of Tutuila, the results of Phase 3 were integrated with results from previous phases of the investigation integral to the formulation of the conceptual model in Phase 2, specifically the resistivity measurements collected during the MT survey and the gas anomalies mapped during the soil gas surveys.

7.1. Integration of Borehole Geology with Resistivity Interpretation

The pattern of resistivity interpreted from the MT survey of the HRZ performed in Phase 2 (Figure 23 and Figure 24) included a low-resistivity (≤10 Ω·m) layer from sea level to -500 meters above sea level (masl) (-1600 ft msl) beneath most of the survey area.

The resistivity pattern illustrated in Figure 24 with horizontal depth slices using the 3D MT inversion, is of sufficient quality to reliably image this zone, despite minor complications from natural and artificial electromagnetic noise.

A low-resistivity zone (conductor) commonly overlies geothermal systems in volcanic settings such as Tutuila, typically forming a low permeability cap due to hydrothermal smectite clay alteration. The low-resistivity zone observed at Tutuila was not necessarily that of a low-permeability hydrothermal clay cap and appeared likely to be saltwater saturated sediments or simply clay-rich low-resistivity volcanogenic sediments. However, it is possible that such low-permeability saltwater saturated sediments could perform the same function as a hydrothermal clay cap (Cumming, 2016; GEOLOGICA, 2014b).

There have been multiple hydrogeologic studies of Tutuila (Eyre and Walker, 1991; Izuka, 1999; Izuka et al., 2007) which have indicated the presence of a buoyant fresh water lens existing above seawater. This subsurface arrangement is typically known as the Ghyben Herzberg (G-H) model, which suggests that fresh water will buoyantly lie 1 foot above sea level for every 40 ft that the fresh water extends below sea level in uniformly distributed, porous reservoir rocks. This means the depth of fresh water, or the top of seawater, can be estimated using the static fresh groundwater elevation. If an aquitard, such as an impermeable clay layer, is present, the G-H model is less effective. The low-resistivity layer indicated by the MT data shows a gradual dip, less than to be expected from a typical G-H surface. Assuming this low-resistivity layer is also a lower permeability layer, this implies both the presence of an aquiclude, affecting Tutuila's hydrogeology, and that the low-resistivity conductor shown by the MT is not simply the result of seawater intrusion and probably consists of clay-rich rocks and/or seawater-saturated clay-rich sediments.

Analysis of the MT results indicate that the base of the low-resistivity zone either dips gently upward to the south or remains mostly flat from inland Tutuila towards the southern coast. This geometry is consistent with the slight up-dip from the center of the island to the coast that could be generated by gravity loading of new volcanic material or the saltwater/fresh-water interface (the G-H relationship). As is apparent in Figure 23, the top of the conductor shows a strong correlation with sea level. The influence of the HRZ is not apparent in the geometry of the conductor, i.e. there is no obvious change in the resistivity in the area of the HRZ.

Fragmental rocks such as tuff, cinder, agglomerate, and volcaniclastic sediments are more easily altered to clay than massive lavas and are therefore more likely to form lithologic conductors. Review of the TGH lithology indicates that there is no direct correlation between either the abundance of fragmental rocks or the logged abundance of clays within the projected conductor interval in TGH-1 and TGH-3. However, the depth interval of the conductor in both wells is characterized by thinly interbedded basaltic lavas and fragmental layers with moderate clay alteration. The case for a lithologic top to the conductor is reasonably good for TGH-3 because basalt lava with weak alteration is dominant until about -60 masl (-200 ft msl), and a more thinly bedded mixed sequence is typical below. This correlation is less clear in TGH-1 where a mixed package is present throughout. These observations indicate that a combination of the thinly interbedded sequence containing clay-rich fragmental rocks and infiltration by seawater produces the conductor.

The thermally conductive gradients observed in both TGHs are consistent with the low-permeability electrical conductor observed in the MT survey. They are also consistent with the findings from the borehole geology including common clay-rich volcaniclastic units and other lithologies with low vertical permeability, though there is high horizontal permeability within fractured lava flows.

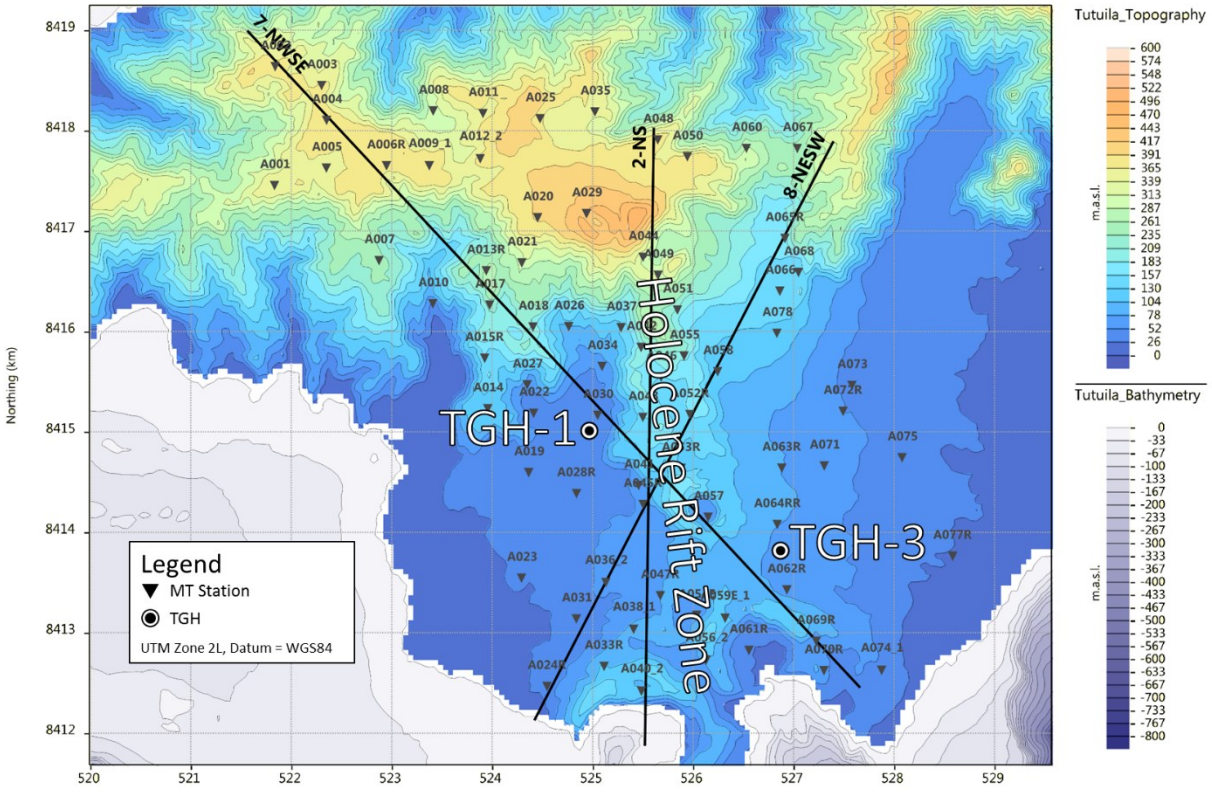

Figure 22: Topographic map of the HRZ in the Tafuna-Leone Plain on SW Tutuila with locations of TGHs, MT stations, and MT-cross section line used below.

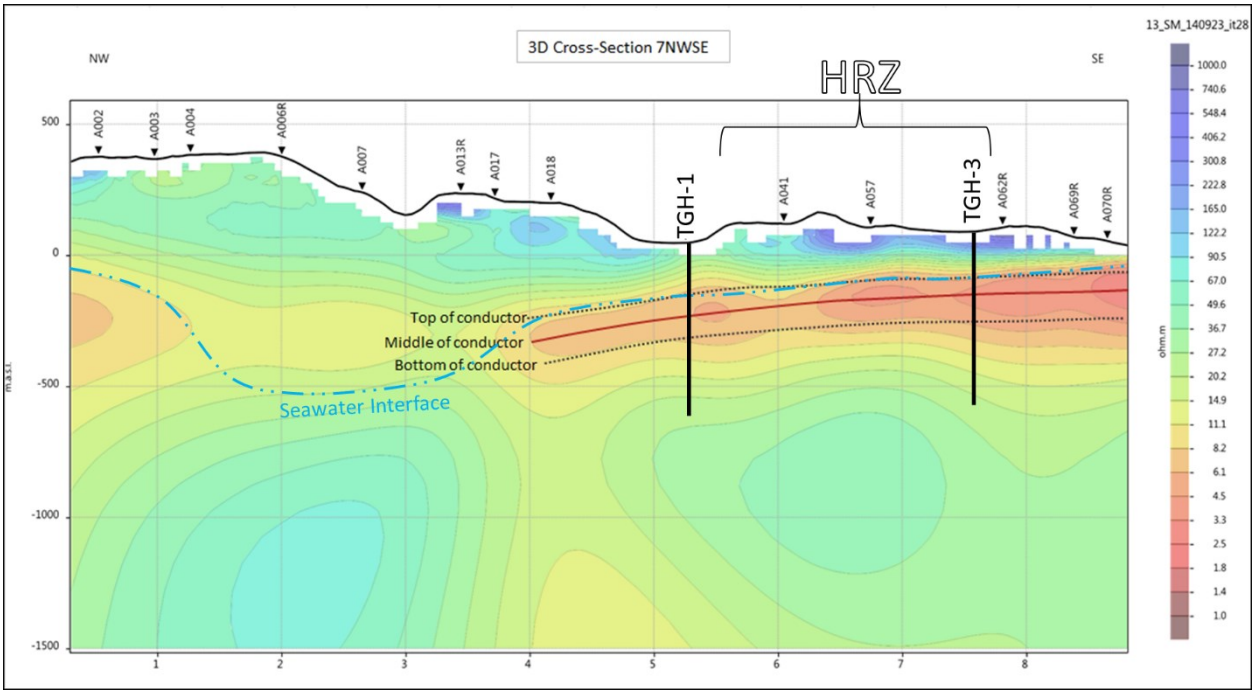

Figure 23. MT cross-section line 7NWSE indicating modeled top, middle, and bottom of the electrical conductor and the correlation with the top of saltwater projected in GEOLOGICA (2014b).

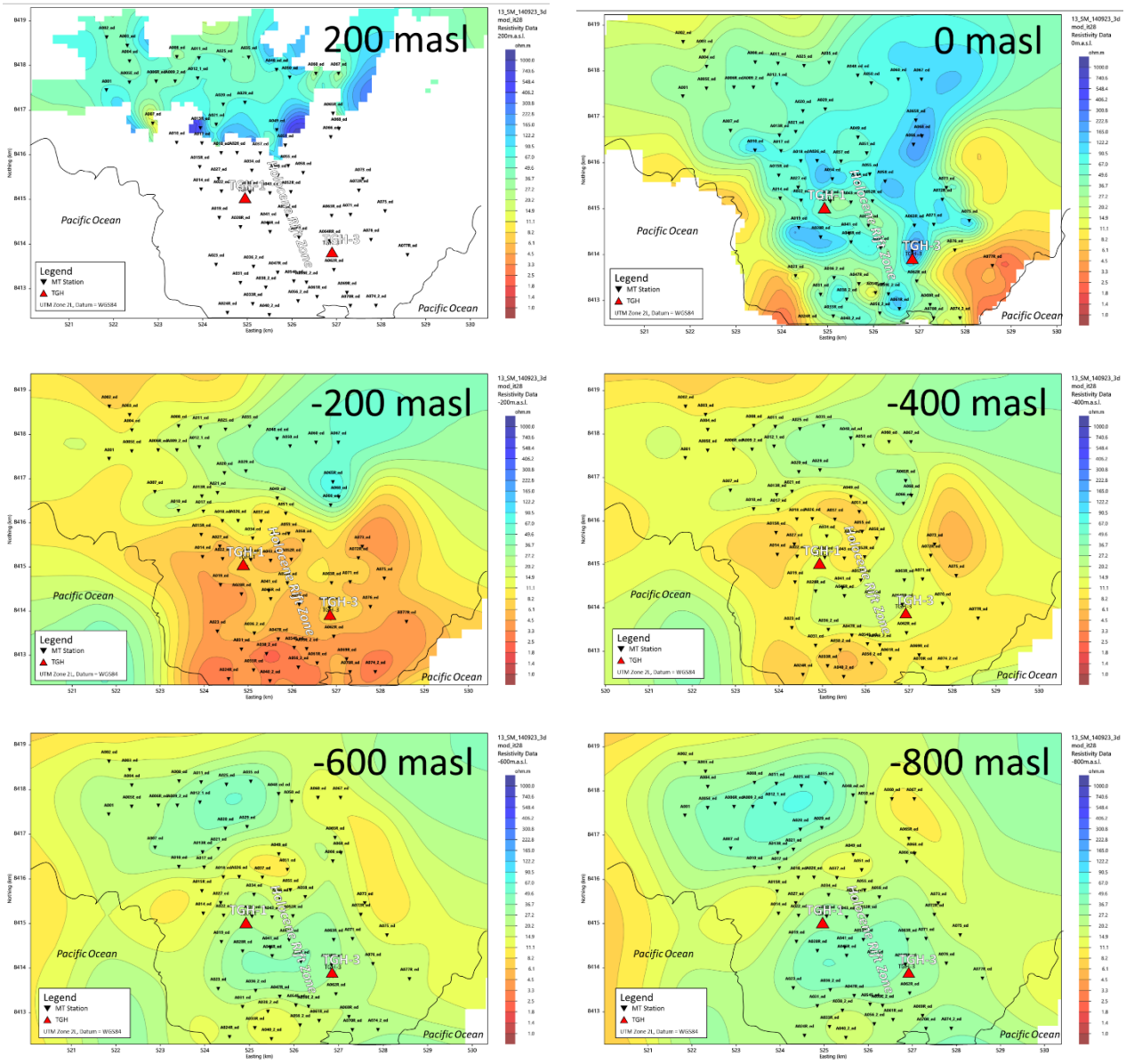

Figure 24. Horizontal sections of 3D modeled resistivity in and around the HRZ at elevations of +200 masl.

7.2. Lithologic Cross Sections

Borehole lithology logged from the core as described above has been integrated with mapped surface geology to produce two lithologic cross sections, AA' and BB' (Figure 25 and Figure 26). The correlation of the borehole lithology logged by GEOLOGICA and the subsurface geology outside of the drilled area was made with reference to Paul Eyre's lithologic cross-sections (Eyre, 2016). Cross sections AA' and BB' are mapped on Figure 3 and displayed in Figure 25 and Figure 26). The lithologic units used in the geologic map (Figure 3) and cross sections (Figure 25 and Figure 26) are correlated below in Table 7.

Table 7. Correlation of Mapped Units with other units used in the cross sections.

Period	Epoch	Epoch Date Range (years B.P.)	Map Unit Pattern	Map Unit (Symbol)	Well Log/ Cross Section Pattern	Cross Section Unit	Unit Description
Quaternery	Holocene	Present to ~11,700		Sedimentary Rocks, Alluvium (Ra)		Leone-derived alluvium (unconsolidated)	Modern soils derived from underlying Leone Volcanics and shed from ridges.
						Taputapu-derived alluvium (unconsolidated)	Talus at the foot of valley walls and river deposited alluvium on valley floors (Stearns, 1944; NPS, 2008).
				Leone Volcanics (Rll)		Leone Volcanics (Rll)	Rll contains olivine pahoehoe basalt flows (Stearns, 1944; NPS, 2008).
				Leone Volcanics - Stony ash (Rla)		Leone Volcanics - Stony ash (Rla)	Rla contains deposits of stony ash along the source fissure zone (Stearns, 1944; NPS, 2008).
				Leone Volcanics - cinder cone (Rlc)		Leone Volcanics - cinder cone (Rlc)	Rlc consists of cinder cone deposits localized at the upper (northern) end of the source fissure (Stearns, 1944; NPS, 2008).
				Leone Volcanics - lithic/vitric (Rlt)		Leone Volcanics - lithic/vitric (Rlt)	Rlt contains at least 2 thick tuff beds from Vailoatai, Fagatele, and Fogamaa Craters with material from Fogamaa Crater atop the Fagatele Crater volcanic deposits (Stearns, 1944; NPS, 2008).
				[No surface outcrops]		Leone Carbonates + Volcanics	Shallow carbonate reefs and marly clays interbedded with Leone Formation lava flows and volcaniclastics. Formed when sea levels rose ~400 ft at beginning of Holocene (Eyre, 2016).
	Pleistocene	~11,700 to 1.8 Million		[No surface outcrops]		Pleistocene Carbonates + Sediments	Pleistocene reef and sediment platform built on the flank of Taputapu volcano, growing towards the ocean surface as Tutuila subsided ~2,500 ft. The material is both depositional (terrigenous and marine) and wave-cut, depending on the changing relationship between fluctuating Pleistocene sea levels with the shoreline of the subsiding island (Eyre, 2016).
				Taputapu Volcanics (Po)		Subaerial Taputapu	Undifferentiated olivine basalts (2 to 15 m thick), dipping 5°- 10° from a rift zone parallel to the Samoan Ridge interlayered with thin- bedded cinder cone deposits, dikes, and thin vitric tuff beds. In some areas the volcanics are capped by thicker flows of porphyritic and nonporphyritic olivine poor basalts. Some red vitric tuff and cinders present locally (Stearns, 1944; NPS, 2008). Subaerial-erupted flank of the Taputapu volcano, including a thin layer of associated sediments. Subsidence during and following the formation of the island submerged these flanks to about 2,500 feet below sea level (Eyre, 2016).
Neogene	Pliocence	~2.6 to 5.3 Million				Submarine Taputapu	Not observed at surface or in core. Submarine-erupted flank of the Taputapu volcano (Eyre, 2016).

B.P. = Before Present

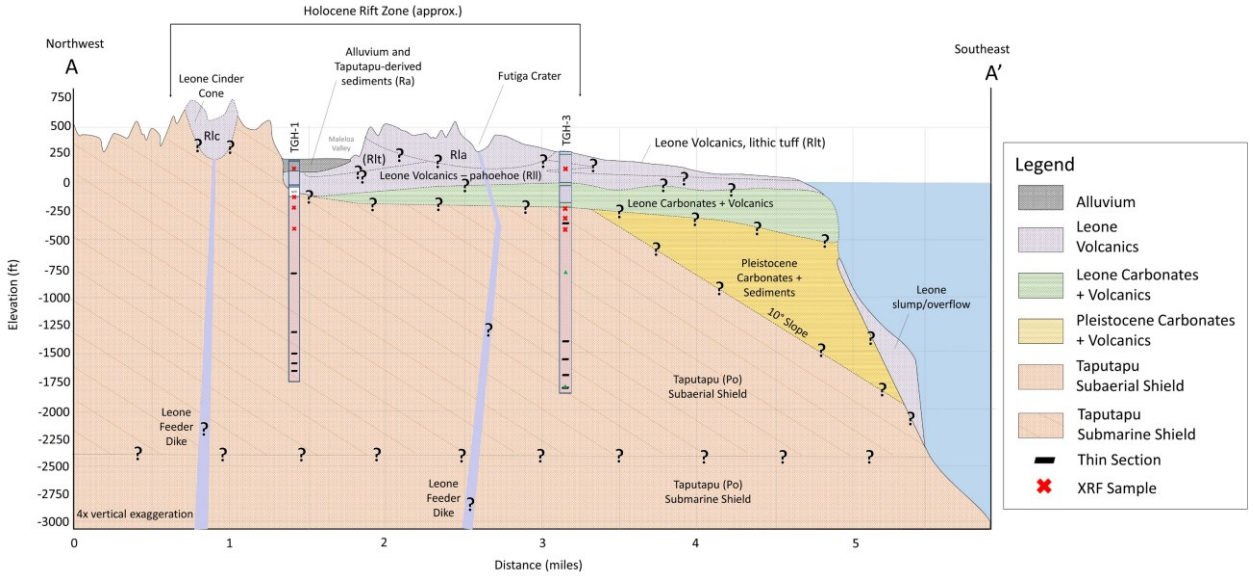

Figure 25. Lithologic Cross Section AA'. Lithology outside drilled area after Eyre (2016). See Figure 3 for section line in map view.

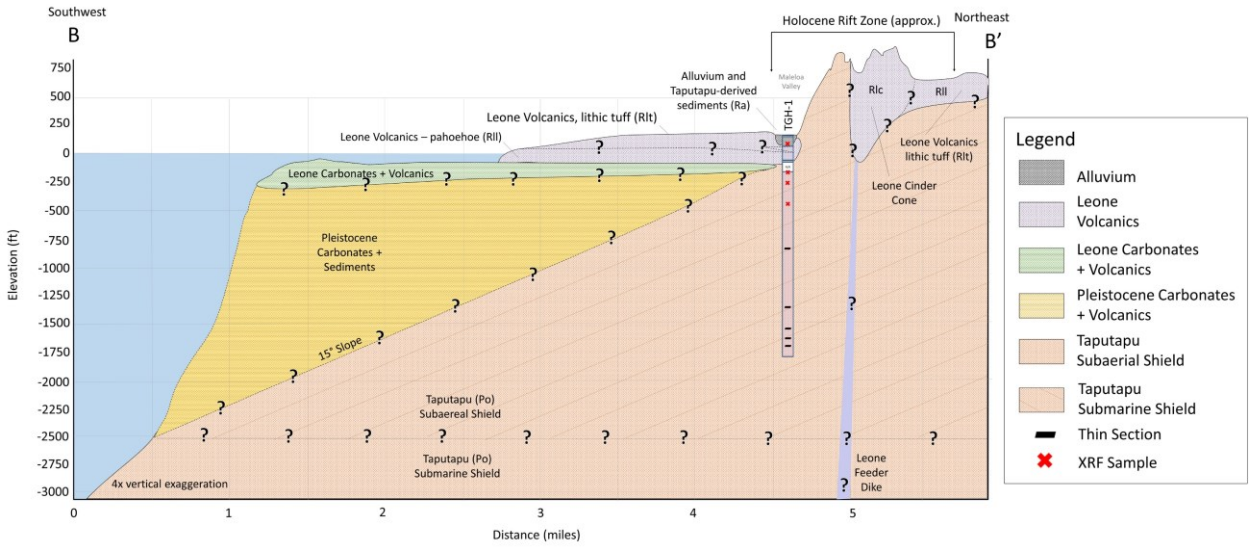

Figure 26. Lithologic Cross Section BB'. Lithology outside drilled area after Eyre (2016). See Figure 3 for section line in map view.

7.3. Gas Anomaly Interpretation – CO_2 and Radon

Carbon dioxide and radon gas concentrations were mapped in association with lineaments and faults on the Tafuna-Leone Plain and in the Holocene Rift Zone during Phase 1 site investigations (Figure 27). Anomalous gas concentrations were identified in several areas adjacent to the HRZ as possible outgassing from deep lateral outflows of a geothermal system upflowing within the axis of the HRZ. TGH-1 and TGH-3 both were sited in part to test this hypothesis since a relatively shallow outflow of a deep blind system would have a better chance of being discovered by a shallow exploration well.

The cold and conductive temperature gradients measured in the two TGHs indicate that these gases are not related to an active geothermal system. The most likely non-biogenic sources of the gas anomalies are very deep crustal sources that exploit the vertical permeability of the HRZ to reach the surface.

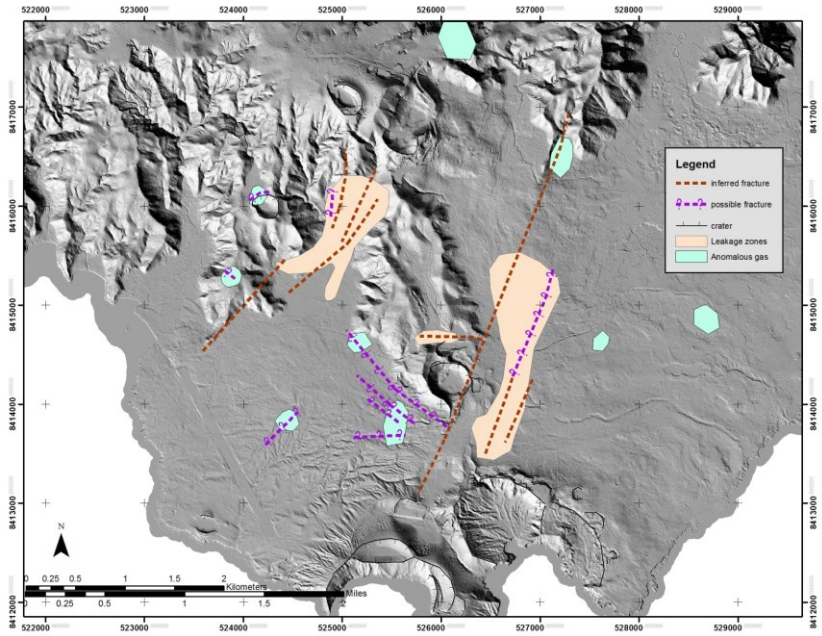

Figure 27. Hillshade image of Holocene Rift Zone showing potential geothermal/magmatic leakage zones and mapped fractures related to leakage and Phase 1 lineament mapping (GEOLOGICA, 2014b). Basemap is LiDAR topographical model from Phase 1.

8. CONCEPTUAL MODEL OF THE HRZ

The geothermal energy investigation of American Samoa has been guided by the principle that for an exploitable geothermal system to exist, four resource attributes must coexist in sufficient abundance: 1) temperature (heat source); 2) permeability; 3) water (reservoir fluid); and 4) an impermeable reservoir cap. These attributes, which could support a geothermal system, must also fit together into a reasonable conceptual model of a geothermal system.

The conceptual model of a geothermal system in the vicinity of the HRZ, should it be present, was developed in Phase 2 and included: 1) the presence of young volcanics indicating a potential heat source; 2) a rift structure indicating the presence of high-angle normal faults that could provide deep permeability; 3) abundant meteoric groundwater recharge and proximity to the sea which provide a source of water to resupply reservoir fluid; and 4) the presence of a conductive layer at depth that could act as an impermeable cap to constrain the reservoir and insulate it from colder intrusion from above. This section describes how the new data updates the conceptual model and affects the geothermal resource potential of the HRZ. The conceptual model is presented in two cross sections, AA' and BB', which have been constructed through the TGHs and the HRZ. Cross section lines are shown on the map in Figure 3. Cross sections are presented in Figure 29 and Figure 30.

These cross sections are scaled and the lithological formation contacts, aquifers, and static temperatures measured in the two boreholes are accurately displayed. Projections of these data sets are necessarily uncertain but are informed by similar geology in other areas and experience with other geothermal systems. Subsurface features depicted, such as buried HRZ faults and the location of dikes and volcanic conduits, are conceptual and not intended to represent actual specific locations of these features. Extrapolation of the lithological contacts beyond the two boreholes was aided by reference to cross sections in Eyre (2016).

8.1. Temperature and Heat Source

Temperatures in the two TGHs are low and nearly identical, and the gradients are similarly low and conductive, indicating no hydrothermal convection indicative of a geothermal system occurs near, or between, the boreholes. Minor differences at shallow depths (<1000 ft bgs) indicate cold meteoric water movement from the highlands. Temperature-depth contours extrapolated from the TGHs are presented in the conceptual model cross sections and are presented below in Table 8.

Table 8. Temperature contour depth information from equilibrated borehole temperature logs.

Well		Temperature at Depth, (°C)				Depth at Temperature, (ft)		
	Max. Temp. (°C)	500 ft	1000 ft	1500 ft	2000 ft	30°C	35°C	40°C
TGH-1	37.1	26.4	29.6	32.8	36.5	1050	1800	2500*
TGH-3	36.9	29.4	31.8	34	36.8	25, 600	1650	2600*

*Projected

Conductive temperature gradients indicate that heat flows by conduction from normal-temperature oceanic crust and through the volcanic basement of Tutuila. Cold seawater and cold fresh water advect heat laterally away from the HRZ through permeable pathways. Measured TGH temperatures provide no evidence of lasting heat from recent volcanism within the HRZ.

Furthermore, new dating of carbonates within the lower Leone Volcanics from TGH-3 indicates that the lower (older) portions of the Leone Volcanic basalt flows erupted approximately 4,000 to 10,000 years B.P., which means they are sufficiently old to have cooled to background temperatures. Trace quantities of moderate to low-temperature alteration mineralogy could have been produced during the transient heat associated with Leone Volcanic eruptions, rather than from a hydrothermal system.

8.2. Permeability

Permeability in the rocks within the HRZ is highly anisotropic. Vertical permeability is very low due to frequent sub-horizontal layers of clay-rich volcaniclastic sediments, except where high-angle to vertical fractures and faults related to the HRZ cut the stratigraphy or where brittle fractured dikes allow water to move vertically. Horizontal permeability is locally very high where basaltic lava flows are highly fractured, especially in fresh, brittle Leone Volcanic flows and tuffs. Where these zones are discontinuous, they may be laterally confined by clay-rich volcaniclastics. The TGHs were not deep enough to encounter highly fractured hyaloclastites associated with the emergent phase of volcanic islands, however these likely exist at greater depth within the Taputapu Formation.

8.3. Water (Recharge)

Cold-water recharge in the form of abundant rainfall, especially at higher elevations, brings fresh water into the HRZ hosted in permeable, young Leone Volcanics. Vertical dikes may act as conduits for fresh water to penetrate deeper into permeable basalt-hosted reservoirs within impermeable clay-rich sediments. Despite the warm tropical ocean surface waters, the thermocline everywhere in the world decreases rapidly below the shallow epipelagic zone to <10°C at 500 m depth, and <5 °C at 1000 m depth (Figure 28). An

effectively infinite source of very cold seawater with infinite permeability envelops the submerged volcanic edifice of deep sea volcanic islands and underlies the freshwater lens on shore.

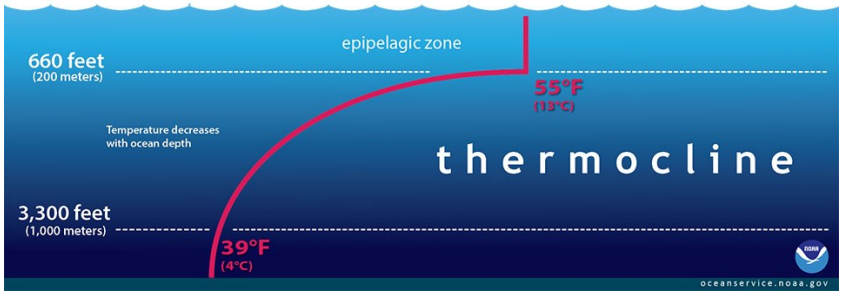

Figure 28. Typical ocean thermocline (NOAA, 2017).

8.4. Reservoir Cap

Detailed analysis of drilling core and cuttings indicates that low-permeability clay-rich layers exist that could provide the necessary vertically impermeable layers needed to cap a reservoir. However, laboratory analyses confirmed that clay alteration is dominantly low-temperature, and the typical moderate-temperature smectite and illite clay alteration associated with active geothermal reservoirs is not present in the necessary abundance to indicate a current geothermal system.

8.5. Updated Conceptual Model

Based on available data prior to drilling, for a geothermal system to exist within the HRZ, the conceptual model postulated hot upflow diverted by clay-rich sediments from ~-500 masl (~-1600 ft msl) to sea level out to a submarine outflow location, explaining the lack of hot springs or other surface geothermal features on land.

In light of the cold and conductive temperatures measured in the two TGHs, the conceptual model has been revised. There does not appear to be an upflow of hot fluid within the HRZ and temperatures are conductive and consistent within the worldwide average of 20-30°C/km up to the shallow groundwater aquifers.

Anomalous gases detected in soil gas flux surveys in and around the HRZ and originally interpreted as potentially sourced from shallow geothermal upflow and lateral outflow are instead likely to be from a much deeper source, possibly magmatic, but unrelated to a geothermal reservoir at practical drilling depths (up to 2.5 miles, or 4 km, for example).

The electrical conductor imaged in the MT is confirmed to be mainly saltwater-saturated, clay-rich volcaniclastic sediments. The finely bedded, alternating stratigraphy of these impermeable sediments with permeable lava flows means that while vertical permeability is very low, horizontal permeability within the lava flows can be very high.

Cold meteoric water (rain) falls on the topographic highlands of Tutuila, quickly infiltrates the permeable young volcanics and flows downgradient under gravity. Within the HRZ, the meteoric water may exploit vertical fractures to form localized deep fault-bounded or dike-impounded groundwater aquifers, seen as temperature reversals in the temperature-depth logs of TGH-3. These aquifers may be drilling targets for groundwater exploration.

Surface cold water could also flow through the vertical fractures of the HRZ and dynamically cool the interior of the rift zone, but this effect is minor given the small surface area.

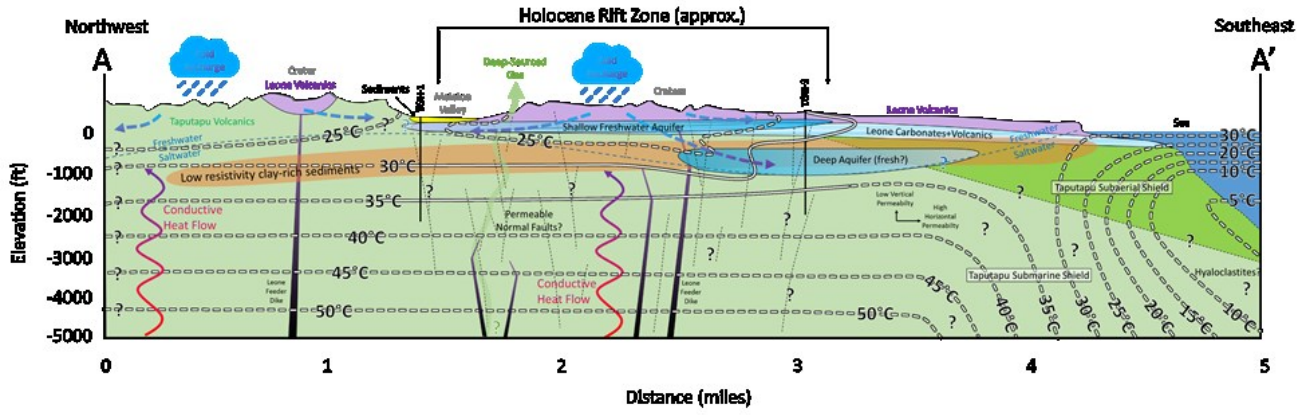

Figure 29. Updated conceptual model of the HRZ along cross section AA'.

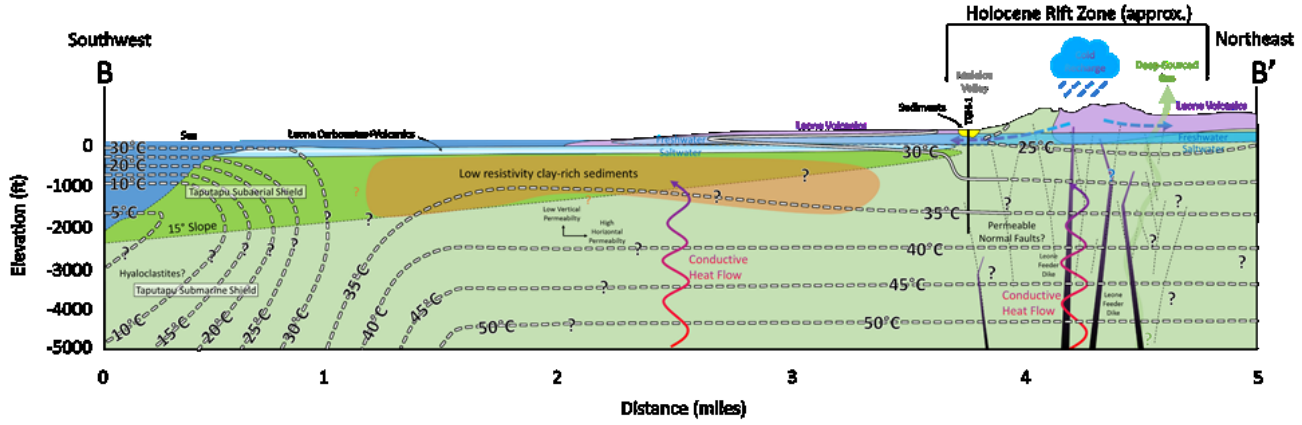

Figure 30. Updated conceptual model of the HRZ along cross section BB'.

8.6. Comparison of Puna, Hawaii and Tutuila

The geothermal field at Puna, Hawaii is a high-temperature, magmatically-heated reservoir contained in a narrow corridor within the East Kilauea Rift Zone (EKRZ) on the flank of the active Kilauea volcano. Reservoir temperatures are over 300°C and reservoir fluid is a mixture of fresh meteoric water from rainfall on the volcanic peaks and seawater infiltrating the EKRZ (Teplow et al, 2009). Based on similarities between Puna and Tutuila (young extensional fault zone, Holocene volcanism, nearby deep cold seawater) Puna was an early analog field for the optimistic case of a geothermal field in the Holocene Rift Zone of Tutuila.

Tutuila has young volcanism less than perhaps 600 years old, however unlike Puna which has experienced volcanic eruptions in the 20th century and is associated with numerous hot springs, there are no thermal features on Tutuila. It was hypothesized that a tightly sealed clay cap (hydrothermally produced and/or composed of marine clays) could protect a blind geothermal system on Tutuila, producing only the anomalous gas fluxes observed in the HRZ. However, the electrical conductor observed at Tutuila does not appear to be the product of hydrothermal alteration whereas Puna does have a hydrothermal clay cap associated with the geothermal system. Puna's clay cap may protect the system from cold seawater flooding. Another difference is that Puna is adjacent to an enormous hydraulic head of fresh water due to the high rainfall, high peaks, and large volume of Hawaii. The island of Hawaii has a subaerial area ~70 times greater than Tutuila and a maximum elevation of ~4200 m compared to 650 m on Tutuila.

Temperature-elevation profiles of TGH-1 and TGH-3, along with those from several deep wells at Puna are shown in Figure 31. TGH-1 and TGH-3 have static temperature gradients similar to the worldwide average of ~25°C/km. Note however that these gradients do not necessarily indicate impermeable rocks given the highly-fractured lava flows encountered to total depth in the cores of both TGHs. Rather they may reflect static saltwater in hydraulic communication with the sea. The Puna wells SOH-1 ad SOH-2 have similar temperatures at depths similar to the bottoms of TGH-and TGH-3 (~35°C at ~-500 masl). In the case of Puna, this is due to an isothermal freshwater aquifer in a highly permeable fractured lava unit. Below this elevation the Puna wells have a high thermal gradient consistent with caprock over a geothermal reservoir. Given the lack of hydrothermal alteration in the core from TGH-1 and TGH-3, there is no reason to expect a sudden similar increase in gradient below this depth on Tutuila.

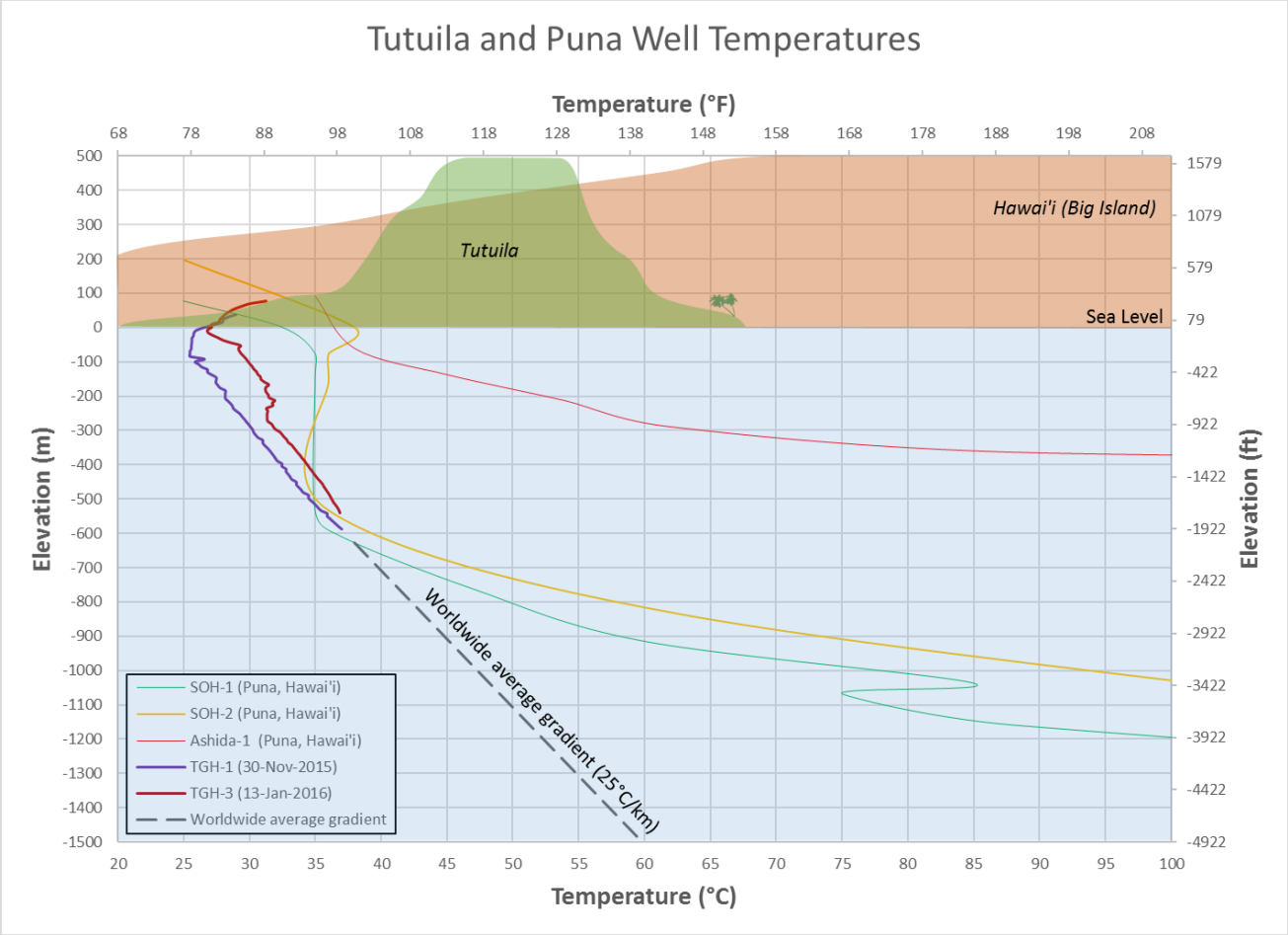

Figure 31. Comparison of temperature vs elevation profiles for wells in Puna, Hawaii and the Tutuila TGHs. Relative size of the islands of Tutuila and Hawaii (Big Island) shown diagrammatically to indicate relative elevation and volume.

9. CONCLUSIONS

9.1. Conclusions specific to the investigation of Tutuila

During Phase 3 of exploration of the geothermal potential of Tutuila, American Samoa, two temperature gradient holes, TGH-1 and TGH-3, were drilled to depths of ~2,200 ft bgs near the HRZ. The geoscientific data collected during this third phase of exploration included:

1. Lithology, alteration mineralogy, textural description and structural observations of rock core (and limited cuttings) from TGH-1 and TGH-3;

2. Whole rock chemistry and petrology of selected samples from TGH-1 and TGH-3 core;

3. Multiple temperature gradient measurements of TGH-1 and TGH-3;

4. Whole rock chemistry, lithology of selected surface samples in the vicinity of the Tafuna-Leone Plain; and

5. Geologic field observations and structural orientations of selected flows observed near the HRZ used to update the geologic map.

Based on the work conducted during this investigation, the following conclusions germane to the geothermal exploration and the geology of Tutuila can be made:

- Rocks found in the two TGHs to depths of ~2,200 ft bgs can be correlated, using visual inspection, with lithologic units mapped at the surface. Previous drilling confirmed the geologic section to less than ~300 ft bgs. Leone Volcanics were observed as interlayered lava flows, tuffs, breccias and other volcaniclastics from 111 to 250 ft bgs in TGH-1 and from 15 to

446 ft bgs in TGH-3. Taputapu Volcanics were observed as interlayered lava flows, tuffs, breccias and other volcaniclastics from 111 to 250 ft bgs in TGH-1 and from 15 to 516 ft bgs in TGH-3.

- In between the last subaerial eruption of the Taputapu shield volcanics and the initial eruption of Leone rejuvenated volcanics, there was a period of erosion which is marked by Taputapu Volcanics-derived paleosols, and at TGH-3, by subsea conditions.
- Carbonates observed in the TGH-3 core from 270 to 299 ft bgs and from 446 to 516 ft bgs indicated that the initial eruptions of Leone Volcanics at the TGH-3 location were probably deposited subsea.
- Preliminary Carbon-14 dates from TGH-3 core samples indicated that the Leone volcanics began to erupt before 10,000 years B.P. and continued at least as recently as ~4,000 years B.P.
- Estimated subsidence rates for Tutuila implied by the depth and ages of carbonates in the TGH-3 core range from -0.74 to 2.43 mm/year for ~7,000 years B.P. to present, consistent with other recent estimates for Upolu.
- Major and minor cation geochemistry previously used to distinguish surface samples of Holocene-age Leone Volcanics from Pleistocene-age Taputapu Volcanics can also be used to distinguish in situ formations in boreholes.
- While trace hydrothermal clay alteration is present in the core, it does not reflect persistent high-temperature conditions nor is it restricted to the low-resistivity layer.
- The low-resistivity layer appears to reflect seawater-saturated sediments without a hydrothermal component.
- In the course of geologic mapping, youthful-looking craters west of Olotele Crater previously mapped as Taputapu Volcanics have been re-mapped as Leone Volcanics.
- A deep, previously unknown aquifer at a depth of ~850 to 1,150 ft bgs in TGH-3 may represent a new groundwater exploration target.
- Permeable high-angle and dip-slip slickensides observed in both TGH cores indicate extensional normal faulting and are the only direct evidence, from either mapped geology or borehole geology, of the extensional stress regime of the HRZ.

These results can be explained by rejuvenated volcanism (Leone Volcanics) producing a Holocene fissure ridge that was flooded with cold fresh water from above and seawater from below. Low temperature gradients and low-temperature alteration are consistent with a deep magmatic source and rapidly cooling narrow pathways for the rejuvenated volcanism allowing the magmas which produced these lavas to cool to background temperatures. The geophysical low-resistivity anomaly is caused by seawater-saturated volcaniclastic rocks with a slightly curved concave-down surface. Carbon dioxide and radon gas anomalies in the HRZ are likely due to deep gases exploiting the vertical permeable conduits of the HRZ.

Despite the young volcanism in the HRZ, the available geoscientific data provide no evidence of an active and exploitable geothermal system.

9.2. Generalized conclusions for geothermal exploration of deep sea volcanic inlands

The investigation of Tutuila has generated conclusions germane to geothermal exploration of deep sea volcanic inlands which may be more generalized, including:

- Interlayered permeable lava flows, impermeable volcaniclastics, fractured hyaloclastites and marine sediments produce a highly anisotropic permeability pattern that interacts with the elevated hydrostatic head of the volcanic edifice and the higher hydrostatic gradient of cold saline seawater to significantly distort the Ghyben Herzberg relationship between seawater and overlying fresh water that often dominates island hydrology.
- High rainfall on high-elevation permeable lavas in a basaltic rift system may find a conduit through underlying lower permeability volcanoclastics with sufficient hydrostatic pressure to push meteoric water toward the ocean at depths of 600 m or more, distorting the Ghyben Herzberg density relationship and chilling rock to at least 600 m below sea level.
- The anisotropic permeability includes high horizontal permeability in fractured lava flows which may allow seawater to move laterally inland at shallower depth than predicted by the Ghyben Herzberg model, especially if aquifers are pumped.
- Fractured lavas and dikes bounded by impermeable clay-bearing volcaniclastic aquitards may host meteoric aquifers both at high elevation and significantly below sea level.

- MT resistivity surveys provide important constraints on the geometry of impermeable clay zones but they are unlikely to resolve resistive vertical conduits related to volcanic necks or fissures that pierce a clay cap at a depth greater than their lateral dimension. The resistivity interpretation near a coastline is made more ambiguous by resistivity variation in freshwater and saltwater saturated aquifers and clay-rich aquicludes.

- Rapid subsidence rates of dormant or extinct volcanic islands commonly complicate interpretations of paleo sea level, correlations of sedimentary facies between boreholes, and implications for geothermal conceptual models.

AKNOWLEDGEMENTS

We would like to thank the American Samoa Power Authority for allowing us to share these results and to the American Samoa Renewable Energy Committee for publishing them.

REFERENCES

Addison, D.J., Tago, T., Toloa, J., Pearthree, E., 2005, Ceramic Deposit Below Fifth to Sixth Century AD Volcanic Ash Fall at Pava'ia'i, Tutuila Island, American Samoa: Preliminary Results from Site AS31-171, New Zealand Journal of Archaeology, 2006, v.27.

Addison, D.J., Ailima, E.L., Hope, V.G., 2014, Late-Holocene Volcanics on Tutuila Island, American Samoa: An Archaeological Perspective on their Chronological and Spatial Distribution. Internal ASPA Report, American Samoa Power Authority. Submitted 24 September 2014.

Cumming, W., and Mackie, R., 2007, MT survey for resource assessment and environmental mitigation at the Glass Mountain KGRA. California Energy Commission, GRDA Geothermal Resources Development Account Report. Available at http://www.energy.ca.gov/2013publications/CEC-500-2013-063/CEC-500-2013-063.pdf, 119 pp.

Cumming, W., 2016, Resource Conceptual Models of Volcano-Hosted Geothermal Reservoirs for Exploration Well Targeting and Resource Capacity Assessment: Construction, Pitfalls and Challenges, Proceedings Stanford Geothermal Workshop.

Davis, D.A., 1962, Ground-Water Reconnaissance of American Samoa, Geologic Survey Water-Supply Paper 1608-C.

Eyre, P.R. Walker, G.P.L., 1991, Geology and ground-water resources of Tutuila, American Samoa, Report prepared for the Government of American Samoa's Environmental Protection Agency, American Samoa Power Authority, and Department of Public Works. Revised February 2016.

Eyre, P.R., 2016, Geologic Cross Sections on the South Side of the Taputapu Volcano, Tutuila, American Samoa. Unpublished report dated June 2016.

GEOLOGICA, 2013, Preliminary Evaluation of the Geothermal Resource Potential of Tutuila Island, American Samoa, unpublished report, dated December 31, 2013.

GEOLOGICA, 2014a, Interim Evaluation of the Geothermal Resource Potential of American Samoa, unpublished report, dated July 24, 2014.

GEOLOGICA, 2014b, Phase 2 Evaluation of the Geothermal Resource Potential of Tutuila Island, American Samoa, unpublished report, dated November 2014.

GEOLOGICA, 2015, Exploration Drilling Plan: Holocene Rift Zone, Tutuila Island, American Samoa, unpublished report, dated January 2015.

GEOLOGICA, 2016a, TGH-1 End-of-Well Summary Report, unpublished report, dated 16 February 2016.

GEOLOGICA, 2016b, TGH-3 End-of-Well Summary Report, unpublished report, dated 16 February 2016.

GEOLOGICA, 2016c, Tutuila Holocene Rift Zone, Phase 3 Geothermal Exploration, Final Report, August 2016. Available at http://www.asrec.net/2016/08/21/tutuila-holocene-rift-zone-phase-3-geothermal-exploration/

Grossman, E.E., Fletcher, C. H., Richmond, B. M., 1998, The Holocene sea-level highstand in the equatorial Pacific: analysis of the insular paleosea-level database, Coral Reefs, 17: 309.

Hart, S.R., Coetzeeb, M., Workman, R.K., Blusztajn, J., Johnson, K.T.M., Sinton, J.M., Steinberger, B., Hawkins, J.W., 2004, Genesis of the Western Samoa seamount province: age, geochemical fingerprint and tectonics, Earth and Planetary Science Letters 227, pp. 37– 56.

Hawkins, J.W., Jr., and Natland, J.H., 1975, Nephelinites and basanites of the Samoan linear volcanic chain: their possible tectonic significance. Earth Planet. Sci. Lett. 24: 427-439.

Hogrefe K.R., 2008, Derivation of Near-shore Bathymetry from Multispectral Satellite Imagery used in a Coastal Terrain Model for the Topographic Analysis of Human Influence on Coral Reefs, M.S. thesis, Oregon State University, Corvallis, OR, pp 116.

Izuka, S.K., 1999, Hydrogeologic interpretations from available ground-water data, Tutuila, American Samoa, Water Resources Investigations, U. S. Geologic Survey: WRI 99- 4064.

Izuka, S.K. Perreault, J.A., Presley, T.K., 2007, Areas Contributing Recharge to Wells in the Tafuna-Leone Plain, Tutuila, American Samoa, U. S. Geologic Survey Investigations Report 2007-5167, 51p.

Keating, B.H., 1992, Geology of the Samoan Islands, In Geology and offshore mineral resources of the Central Pacific Basin, eds. Keating, B.H., B.R. Bolton, 127- 178. New York: Springer.

Konter, J.G., Jackson, M.G., 2012, Tremendous volumes of rejuvenated volcanism in Samoa: Evidence supporting a tectonic influence on late-stage volcanism. Geochem., Geophys., Geosyst. v. 13.

Long, D., Lovell, M.A., Rees, J.G., Rochelle, C.A., 2009, Sediment-hosted Gas Hydrates: New Insights on Natural and Synthetic Systems, Geological Society Special Publication No. 319.

McDougall, I., 1985, Age and Evolution of the Volcanoes of Tutuila, American Samoa, Pacific Science, vol. 39, no. 4.

Mortensen, A. K., & Axelsson, G., 2013, Developing a Conceptual Model of a Geothermal System, 1–10. Short Course on Conceptual Modeling of Geothermal Systems (ISOR).

Natland, J.H., 1980, The progression of volcanism in the Samoan linear volcanic chain. Am. J. Sci., 280A, 709-735.

Natland, J.H. and D.L. Turner, 1985, Age progression and petrological development of Samoan shield volcanoes: Evidence form K-Ar ages, lava compositions, and mineral studies, Geologic Investigations of the Northern Melanesian Borderland, Circum-Pacific Council for Energy and Mineral Resources Earth Science Series, v. 3.

NOAA, 2017, http://oceanservice.noaa.gov/facts/thermocline.html.

Nordquist, J. and Delwiche, B., 2013, The McGinness Hills Geothermal Project. Geothermal Resources Council Transactions, 37, 57-64.

NPS, 2008, National Park of American Samoa, Geologic Resource Evaluation Report, Natural Resource Report, NPS/NRPC/GRD/NRR—2008/025.

Phelan, M., 1999, A ΔR correction value for Samoa from known-age marine shells. Radiocarbon 41(1):99–101.

Pirazzoli, P.A., 1991, World Atlas of Holocene Sea-Level Changes, Elsevier.

Reinhard, A., 2016, 14C dating results from TGH-3, undated and unpublished report.

Sand, C., Bole, J., Baret, D., Ouetcho, A., Petchey, F., Hogg, F., Tautala, A., 2016, Geological subsidence and sinking islands: The case of Manono (Samoa), Archaeology in Samoa, v. 00.

Stearns, H.T., 1944, Geology of the Samoan Islands. Geol. Soc. Am. Bull. 55: 12791332.

Stuiver, M. and Polach, H.A., 1977, Discussion Reporting of 14C Data, Radiocarbon, v. 19, p.355.

Teplow, W., Marsh, B., Hulen, J., Spielman, P., Kaleikini, M., Fitch, D., Rickard, W., 2009, Dacite Melt at the Puna Geothermal Venture Wellfield, Big Island of Hawaii, GRC Transactions, Vol. 33.

US-DOE, 2014, Best practices for Risk Reduction Workshop Follow-up Manual. Published 8-Jul-2014. 40 p.

Ussher, G., Harvey, C., Johnstone, R., Anderson, E., 2000, Understanding the resistivities observed in geothermal systems. Proceedings World Geothermal Congress 2000. 1915-1920.

Wright D.J., Roberts J.T., Fenner D., Smith J.R., Koppers A.P., Naar D.F., Hirsch E.R., Clift L.W., Hogrefe K.R., 2012, Seamounts, ridges, and reef habitats of American Samoa. In: Seafloor geomorphology as benthic habitat: GeoHAB atlas of seafloor geomorphic features and benthic habitats; Harris, P.T. and Baker, E.K.